

# Radiative neutrino masses from dim-7 SMEFT: a simplified multi-scale approach

---

Kåre Fridell<sup>a,b</sup> Lukáš Gráf<sup>c,d,e,f</sup> Julia Harz<sup>g</sup> Chandan Hati<sup>h</sup>

<sup>a</sup>*Theory Center, Institute of Particle and Nuclear Studies,  
High Energy Accelerator Research Organization (KEK), Tsukuba 305-0801, Japan*

<sup>b</sup>*Department of Physics, Florida State University, Tallahassee, FL 32306, USA*

<sup>c</sup>*Nikhef, Theory Group, Science Park 105, 1098 XG Amsterdam, The Netherlands*

<sup>d</sup>*Institute of Particle and Nuclear Physics, Faculty of Mathematics and Physics, Charles University  
in Prague, V Holešovičkách 2, 180 00 Praha 8, Czech Republic*

<sup>e</sup>*Department of Physics, University of California, Berkeley, CA 94720, USA*

<sup>f</sup>*Department of Physics, University of California, San Diego, CA 92093, USA*

<sup>g</sup>*PRISMA<sup>+</sup> Cluster of Excellence & Mainz Institute for Theoretical Physics, FB 08 - Physics,  
Mathematics and Computer Science, Johannes Gutenberg-Universität Mainz, 55099 Mainz, Ger-  
many*

<sup>h</sup>*Instituto de Física Corpuscular (IFIC), Universitat de Valencia-CSIC, E-46980 Valencia, Spain*

*E-mail: [karef@post.kek.jp](mailto:karef@post.kek.jp), [lukas.graf@nikhef.nl](mailto:lukas.graf@nikhef.nl),  
[julia.harz@uni-mainz.de](mailto:julia.harz@uni-mainz.de), [chandan@ific.uv.es](mailto:chandan@ific.uv.es)*

**ABSTRACT:** Lepton-number-violating interactions occur in the Standard Model Effective Field Theory (SMEFT) at odd dimensions starting from the dimension-5 Weinberg operator. Although the operators at dimension-7 and higher are more suppressed by the heavy new scale, they can be crucial when traditional seesaw mechanisms leading to tree-level dimension-5 contributions are absent. We identify all minimal tree-level UV-completions for dimension-7  $\Delta L = 2$  SMEFT operators without covariant derivatives and propose a new simplified approach for estimating the radiative neutrino masses arising from such operators. This dimensional-regularisation-based approach provides a more accurate estimate for the loop neutrino masses when the new physics fields are hierarchical in mass, as compared to the cut-off-regularisation-based approach often employed in the literature. This allows us to identify viable regions of parameter space in the full list of relevant simplified models close to the current limits set by neutrinoless double beta decay and the LHC that would previously have been thought to be excluded by neutrino-mass constraints.

---

## Contents

<b>1</b>	<b>Introduction</b>	<b>1</b>
<b>2</b>	<b><math>\Delta L = 2</math> dimension-7 SMEFT and tree-level UV-completions</b>	<b>3</b>
<b>3</b>	<b>Neutrino masses without tree-level dim-5 Weinberg operator</b>	<b>8</b>
<b>4</b>	<b>Loop neutrino masses: cut-off EFT estimates vs. exact UV results</b>	<b>11</b>
4.1	Single-scale EFT estimate based on cutoff regularisation	11
4.2	An explicit UV model example and exact loop computation	12
<b>5</b>	<b>A simplified multi-scale approach to loop neutrino masses</b>	<b>15</b>
5.1	Simplified multi-scale formalism for one-loop neutrino masses	17
5.2	Simplified multi-scale formalism for two-loop neutrino masses	19
5.3	Generalised simplified multi-scale results for radiative neutrino masses	21
<b>6</b>	<b>Phenomenology of UV-completions at dimension-7</b>	<b>23</b>
<b>7</b>	<b>Conclusions</b>	<b>28</b>
<b>A</b>	<b>Covariant derivative expansion</b>	<b>29</b>
A.1	Scalar field	30
A.2	Fermion field	30
A.3	Vector field	32

---

## 1 Introduction

The observation of non-zero neutrino masses represents a key laboratory evidence for beyond-the-Standard-Model (BSM) physics. Possible theoretical explanations can be used as guidance in searches for new, UV degrees of freedom. If neutrinos are Majorana particles, the corresponding New Physics (NP) model inevitably needs to include interactions that do not preserve the lepton number. Therefore, observables testing this seemingly accidental global symmetry of the Standard Model (SM) provide a well-motivated probe of BSM scenarios.

At low energies, the NP effects can be encoded in terms of the effective operators invariant under the SM gauge symmetry, forming the Standard Model Effective Field Theory (SMEFT). Lepton number violation (LNV) occurs in this formalism at odd mass dimensions [1]. Therefore, the leading contribution is expected to stem from dimension-5 SMEFT consisting of the well-known Weinberg operator. The set of next-to-leading LNV interactions appear at dimension 7, the basis of which has been established not so long ago [2–7].

In Ref. [8] we have discussed the phenomenological limits on dimension-7  $\Delta L = 2$  operators. These operators are constrained by a wide range of different searches, including e.g. the LHC,  $0\nu\beta\beta$  decay, and rare kaon decays [8]. However, as pointed out therein, the effective approach is subject to a number of assumptions that may result in limited validity and possibly less realistic constraints in comparison with specific UV-completions. To counter these issues we continue our investigation of dimension-7  $\Delta L = 2$  operators in this work by analysing the complete set of simplified models with up to two new fields that UV-complete these non-renormalisable interactions at tree-level (see also Ref. [9]).

Despite their stronger suppression compared to the dimension-5 (Weinberg) operator, LNV at dimension 7 in SMEFT can also lead to sizable contributions for specific lepton-number-violating processes. Clearly, if the usual three seesaw fields leading to type-I, type-II, or type-III seesaw mechanisms are absent at high energies, the Weinberg operator is not generated at tree-level at low energies. In such a scenario, the leading contribution to LNV may stem from dimension-7 operators, which is a possibility previously proposed and discussed in a variety of publications [9–22]. Observations suggesting a higher-dimensional origin of LNV could hint at radiative neutrino Majorana mass models (see e.g. Refs. [23, 24]).

When determining the neutrino mass contributions within the EFT framework, typically the cut-off-regularisation-based estimates are often employed in literature, see e.g. Ref. [25] for some relevant discussion on the methodology. It can be easily seen from a direct comparison with neutrino mass expressions obtained in complete UV models, these simple estimates suffer from a number of caveats stemming from the assumptions necessary for application of the naive cut-off approximation. The most apparent discrepancy occurs in case of a large hierarchy between the masses of the new fields. In this work we address these drawbacks and study the loop neutrino masses from UV physics underlying the dimension-7 SMEFT. We propose a simplified approach based on dimensional regularisation and matching simple UV-completions to an intermediate EFT. This helps in getting a much closer approximation of the exact model-based results in contrast to the simple cut-off regularisation based estimates, when the heavy NP is hierarchical in mass. Allowing for the masses of the UV fields to be independent parameters opens up new parts of parameter space to be explored, which we use to derive neutrino-mass constraints in the simplified multi-scale approach setup and confront them with bounds from other relevant observables.

The paper is organized as follows: we review the EFT framework and list all the possible two-field UV-completions using the systematic approach of covariant derivative expansion (see Appendix A for details of the calculation) in Section 2. Next, we cover the neutrino mass generation mechanisms in all the listed UV-completions of the dimension-7 operators in Section 3, and provide an explicit comparison of neutrino masses obtained as a single-scale cut-off estimate with a full in-depth analysis of the SM extension with two scalar leptoquarks,  $\tilde{R}_2$  and  $S_1$  in Section 4.2. Following that we introduce and discuss a multiscale EFT approach to radiative neutrino masses in Section 5. Eventually, we combine, compare, and analyse the constraints imposed on the studied simplified models by neutrino masses as well as other available observables in Section 6, before we conclude in Section 7.

Type	$\mathcal{O}$	Operator
$\Psi^2 H^4$	$\mathcal{O}_{LH}^{pr}$	$\epsilon_{ij}\epsilon_{mn}(\overline{L}_p^{ci}L_r^m)H^jH^n(H^\dagger H)$
$\Psi^2 H^3 D$	$\mathcal{O}_{LeHD}^{pr}$	$\epsilon_{ij}\epsilon_{mn}(\overline{L}_p^{ci}\gamma_\mu e_r)H^j(H^m i D^\mu H^n)$
$\Psi^2 H^2 D^2$	$\mathcal{O}_{LHD1}^{pr}$	$\epsilon_{ij}\epsilon_{mn}(\overline{L}_p^{ci}D_\mu L_r^j)(H^m D^\mu H^n)$
	$\mathcal{O}_{LHD2}^{pr}$	$\epsilon_{im}\epsilon_{jn}(\overline{L}_p^{ci}D_\mu L_r^j)(H^m D^\mu H^n)$
$\Psi^2 H^2 X$	$\mathcal{O}_{LHB}^{pr}$	$g\epsilon_{ij}\epsilon_{mn}(\overline{L}_p^{ci}\sigma_{\mu\nu}L_r^m)H^jH^n B^{\mu\nu}$
	$\mathcal{O}_{LHW}^{pr}$	$g'\epsilon_{ij}(\epsilon\tau^I)_{mn}(\overline{L}_p^{ci}\sigma_{\mu\nu}L_r^m)H^jH^n W^{I\mu\nu}$
$\Psi^4 D$	$\mathcal{O}_{\bar{d}uLLD}^{prst}$	$\epsilon_{ij}(\overline{d}_p\gamma_\mu u_r)(\overline{L}_s^{ci}iD^\mu L_t^j)$
$\Psi^4 H$	$\mathcal{O}_{\bar{e}LLLH}^{prst}$	$\epsilon_{ij}\epsilon_{mn}(\overline{e}_p L_r^i)(\overline{L}_s^{cj}L_t^m)H^n$
	$\mathcal{O}_{\bar{d}LueH}^{prst}$	$\epsilon_{ij}(\overline{d}_p L_r^i)(\overline{u}_s^c e_t)H^j$
	$\mathcal{O}_{\bar{d}LQLH1}^{prst}$	$\epsilon_{ij}\epsilon_{mn}(\overline{d}_p L_r^i)(\overline{Q}_s^{cj}L_t^m)H^n$
	$\mathcal{O}_{\bar{d}LQLH2}^{prst}$	$\epsilon_{im}\epsilon_{jn}(\overline{d}_p L_r^i)(\overline{Q}_s^{cj}L_t^m)H^n$
	$\mathcal{O}_{\bar{Q}uLLH}^{prst}$	$\epsilon_{ij}(\overline{Q}_p u_r)(\overline{L}_s^c L_t^i)H^j$

**Table 1:** List of all independent  $\Delta L = 2$  operators at dimension-7 SMEFT extracted from the basis of Ref. [26, 27]. Here,  $D_\mu x^n$  denotes  $(D_\mu x)^n$  for  $x \in \{L_i, H\}$ .

## 2 $\Delta L = 2$ dimension-7 SMEFT and tree-level UV-completions

With NP expected to be present at energy scales higher than that of electroweak symmetry breaking, it has become customary to view and treat the SM as an effective description of a UV-complete theory. In this picture the low-energy SM Lagrangian can be extended by a corresponding effective part as

$$\mathcal{L} = \mathcal{L}_{\text{SM}} + \mathcal{L}_{\text{eff}}, \quad (2.1)$$

where

$$\mathcal{L}_{\text{eff}} = \sum_d \sum_a C_a^{(d)} \mathcal{O}_a^{(d)}, \quad (2.2)$$

with  $C_a^{(d)}$  denoting the Wilson coefficients of the respective effective operators  $\mathcal{O}_a^{(d)}$  of mass dimension  $d$ . Operators that contribute to Majorana neutrinos masses must violate lepton number  $L$  by two units,  $\Delta L = 2$ , and they appear only at odd mass dimensions. Therefore, the Lagrangian we consider in this work reads

$$\mathcal{L}_{\text{eff}} = C^{(5)} \mathcal{O}^{(5)} + \sum_a C_a^{(7)} \mathcal{O}_a^{(7)} + \sum_a C_a^{(9)} \mathcal{O}_a^{(9)} + \dots \quad (2.3)$$

We focus specifically on dimension-7 operators, following the notation used in Ref. [8]. For clarity, we show explicitly the definition of the whole  $\Delta L = 2$  dimension-7 SMEFT basis in Tab. 1.

We can expand the operators in Tab. 1 following the procedure of Ref. [18], which we

extend by including heavy vector fields. Using the covariant derivative expansion (CDE) formalism [28], we identify the dimension-7 LNV operators in Tab. 1 with the terms found by systematically integrating out heavy BSM fields from a renormalisable Lagrangian. This lets us find all possible tree-level UV-completions of the dimension-7 LNV operators. In Sec. 6 we use this method to expand upon the results of previous works [9–22] by systematically categorizing the UV-completions in terms of their corresponding operators, evaluating the neutrino masses for each model, and comparing these results with a wide set of phenomenological probes for a varying hierarchy in the internal degrees of freedom.

We start with a general Lagrangian  $\mathcal{L}_S$  describing a simplified model extension to the SM,

$$\mathcal{L}_S = \sum_i (\mathcal{L}_{\pi_i}^{\text{kin}} + \mathcal{L}_{\pi_i}^{\text{int}} + \mathcal{L}_{\Pi_i}^{\text{kin}} + \mathcal{L}_{\Pi_i}^{\text{int}}) . \quad (2.4)$$

Here  $\pi_i$  is a light field, which in our case will correspond to the different fields of the SM, and  $\Pi_i$  is a heavy field  $m_{\Pi_i} \sim \Lambda_{\text{NP}}$  belonging to a NP extension, which can correspond to a scalar  $\Phi_i$ , fermion  $\Psi_i$  or vector  $V_i$ . The superscript *kin* denotes kinetic terms and *int* interaction terms, where the last term in Eq. (2.4) also includes the interactions between heavy and light fields. By assuming that we are only interested in observable phenomena below some heavy scale  $\Lambda_{\text{NP}}$ , we may rewrite the interaction Lagrangian involving heavy fields in terms of effective operators  $\mathcal{L}_{\Pi_j}^{\text{int}} \rightarrow \mathcal{L}_{\text{eff}}$  where  $\mathcal{L}_{\text{eff}}$  corresponds to the EFT Lagrangian given in Eq. (2.3). This replacement can be done via covariant derivative expansion (CDE) (for details see Appendix A), in which we take the derivative of a general interaction Lagrangian with respect to a heavy field [18, 28]

$$\frac{\partial \mathcal{L}_{\Pi_i}^{\text{int}}}{\partial \Pi_i^\dagger} = \sum_{j,a,b,c} \left( 1 + c^{\Pi_j} \frac{\partial \mathcal{L}_{\Pi_j}^{\text{int}}}{\partial \Pi_j^\dagger} \right) (c_2^\pi \pi_a \pi_b + c_3^\pi \pi_a \pi_b \pi_c) , \quad (2.5)$$

where  $c^{\Pi_i}$  has mass dimension  $d = 3$ , and  $c_2^\pi, c_3^\pi$  have the appropriate mass dimensions depending on whether the light fields  $\pi_i$  are fermions or bosons<sup>1</sup>. To end up with a Lagrangian with only light fields, Eq. (2.5) can then be applied again onto itself by expanding the term with the remaining derivative  $\partial \mathcal{L}_{\Pi_j}^{\text{int}} / \partial \Pi_j^\dagger$  in the same way, repeating this step until only light fields remain. This fully light Lagrangian can then be implemented in the expansions shown below in order to obtain a series of effective operators. For a scalar field we have the effective Lagrangian [18, 28]

$$\mathcal{L}_{\text{eff}}^\Phi = \frac{\partial \mathcal{L}_\Phi^{\text{int}}}{\partial \Phi} \left( \frac{1}{m_\Phi^2} - \frac{D^2}{m_\Phi^4} + \dots \right) \frac{\partial \mathcal{L}_\Phi^{\text{int}}}{\partial \Phi^*} . \quad (2.6)$$

For Dirac fermions we have [18, 28]

$$\mathcal{L}_{\text{eff}}^\Psi = \frac{\partial \mathcal{L}_\Psi^{\text{int}}}{\partial \bar{\Psi}} \left( \frac{1}{m_\Psi^2} + \frac{D^2 + \frac{1}{2} X_{\mu\nu} \sigma^{\mu\nu}}{m_\Psi^4} + \dots \right) (i \not{D} + m_\Psi) \frac{\partial \mathcal{L}_\Psi^{\text{int}}}{\partial \Psi} , \quad (2.7)$$

---

<sup>1</sup>Note that the term with  $c_3^\pi$  is only meaningful if all of the fields  $\pi_a, \pi_b$ , and  $\pi_c$  are bosons.

where  $\sigma^{\mu\nu} \equiv \frac{i}{2} [\gamma^\mu, \gamma^\nu]$  corresponds to a tensor current, and where  $X_{\mu\nu}$  is the field strength of a gauge field corresponding to the covariant derivative  $D$ . The relation for Majorana fermions can be obtained via the replacement  $m_\Psi \rightarrow \frac{1}{2}m_\Psi$ . Lastly, for vector fields we have

$$\mathcal{L}_{\text{eff}}^V = \frac{\partial \mathcal{L}_V^{\text{int}}}{\partial V^\mu} \left( \frac{\eta^{\mu\nu}}{m_V^2} + \frac{D^2 \eta^{\mu\nu} - D^\mu D^\nu}{m_V^4} + \dots \right) \frac{\partial \mathcal{L}_V^{\text{int}}}{\partial V^{\nu*}}. \quad (2.8)$$

For each dimension-7  $\Delta L = 2$  SMEFT operator, we systematically combine the SM fields in pairs and read off the corresponding representation under the SM gauge group for each combination. This then corresponds to the representation of a NP field that would couple to this pair in a vertex belonging to a NP interaction Lagrangian. In turn, this NP field can then be paired with the remaining SM fields until only renormalisable terms are left, at which point we identify the sum of these terms with the interaction Lagrangian that is our starting point in the CDE. By systematically repeating this procedure we obtain a list of all possible tree-level UV-completions. This lets us match each operator to a finite set of tree-level UV-completions, including operators with derivatives. We limit ourselves to tree-level UV-completions in this work.

In Tab. 2 we list the different BSM fields that appear in the tree-level UV-completions of the dimension-7  $\Delta L = 2$  operators. Here the representation of each field is shown with respect to the SM gauge group  $SU(3)_c \times SU(2)_L \times U(1)_Y$ , and  $S$ ,  $F$ , and  $V$  denote whether the field is a scalar, fermion, or vector, respectively. The rightmost column shows the different couplings to the SM fields, where  $\tilde{H} = i\sigma_2 H^*$ . Each UV-completion consists of two fields, such that a field in the left gray column should be combined with a single field from one of the cells in the corresponding row. Note that two or more BSM fields can also couple to each other in a single vertex. Note also that  $F_4$  does not have any coupling to only SM fields. It appears in a UV-completion of  $\mathcal{O}_{LH}$  together with  $\Sigma$ , which  $F_4$  can couple to together with the Higgs. This UV-completion then involves two instances of  $\Sigma$  such that the whole diagram resembles that of inverse seesaw.

In Tab. 3 we show the different combinations of BSM fields from Tab. 2 that lead to tree-level UV-completions of the dimension-7  $\Delta L = 2$  operators. Here the field shown in the leftmost column can be combined with one of the other fields of the same row to realize the operator shown at the top of the corresponding column.

In this work we only consider UV-completions for seven out of the original twelve dimension-7  $\Delta L = 2$  operators, namely those of types  $\Psi^4 H$ ,  $\Psi^2 H^4$ , and  $\Psi^2 H^3 D$ . As can be seen from Tab. 1, operators that contain  $D^2$  or  $X$  can be understood as higher order corrections to a lower-dimensional operator, which in our case would correspond to the dimension-5 operator. Furthermore, as was noted in Ref. [18], since the  $\Psi^4 D$ -type operator  $\mathcal{O}_{\bar{d}uLLD}$  contains a single covariant derivative, it must originate from a UV-completion containing a fermion mediator, c.f. Eq. (2.7). However, since it has four external fermion legs, there is no such UV-completion at tree-level, and we conclude that no such tree-level UV-completion is possible for this operator.

In what follows we still aim to focus on UV-completions that do not also lead to the dimension-5 operator at tree-level, since if this operator is induced it would likely dominate over any dimension-7 contribution. Note that even when it comes to the considered

Field	Rep	Coupling to SM fields (+h.c.)
$\mathcal{S}$	$S(1, 1, 0)$	$\frac{1}{2}\kappa_{\mathcal{S}}\mathcal{S}H^\dagger H + \frac{1}{2}\lambda_{\mathcal{S}}\mathcal{S}\mathcal{S}H^\dagger H$
$\Xi$	$S(1, 3, 0)$	$\frac{1}{2}\kappa_{\Xi}H^\dagger\Xi^a\sigma^a H + \frac{1}{2}\lambda_{\Xi}(\Xi\Xi)(H^\dagger H)$
$h$	$S(1, 1, 1)$	$y_h h^\dagger \bar{L}i\sigma_2 L^c + \kappa_h h^\dagger \tilde{H}^\dagger H$
$\Delta$	$S(1, 3, 1)$	$\frac{1}{4}\lambda_{\Delta}(\Delta^\dagger\Delta)(H^\dagger H) + \frac{1}{4}\lambda'_{\Delta}f_{abc}(\Delta^{a\dagger}\Delta^b)(H^\dagger\sigma^c H)$ $+ y_{\Delta}\Delta^{a\dagger}\bar{L}\sigma^a i\sigma_2 L^c + \kappa_{\Delta}\Delta^{a\dagger}(\tilde{H}^\dagger\sigma^a H)$
$\varphi$	$S(1, 2, 1/2)$	$\lambda_{\varphi}(\varphi^\dagger H)(H^\dagger H) + y_{\varphi}^e\varphi^\dagger\bar{e}L + y_{\varphi}^d\varphi^\dagger\bar{d}Q + y_{\varphi}^u\varphi^\dagger i\sigma_2\bar{Q}^T u$
$\Theta_1$	$S(1, 4, 1/2)$	$\lambda_{\Theta_1}(H^\dagger\sigma^a H)C_{ab}^I\tilde{H}^b\epsilon_{IJ}\Theta_1^J$
$\Theta_3$	$S(1, 4, 3/2)$	$\lambda_{\Theta_3}(H^\dagger\sigma^a\tilde{H})C_{ab}^I\tilde{H}^b\epsilon_{IJ}\Theta_3^J$
$S_1$	$S(\bar{3}, 1, 1/3)$	$y_{S_1}^{ql}S_1\bar{Q}^c i\sigma_2 L + y_{S_1}^{qq}S_1\bar{Q}i\sigma_2 Q^c + y_{S_1}^{du}S_1\bar{d}u^c + y_{S_1}^{eu}S_1\bar{e}u^c$
$\tilde{R}_2$	$S(3, 2, 1/6)$	$y_{\tilde{R}_2}\tilde{R}_2^\dagger i\sigma_2 \bar{L}^T d$
$S_3$	$S(\bar{3}, 3, 1/3)$	$y_{S_3}^{ql}S_3^a\bar{Q}^c i\sigma_2\sigma^a L + y_{S_3}^{qq}S_3^a\bar{Q}\sigma^a i\sigma_2 Q^c$
$N$	$F(1, 1, 0)$	$\lambda_N\bar{N}\tilde{H}^\dagger L$
$\Sigma$	$F(1, 3, 0)$	$\frac{1}{2}\lambda_{\Sigma}\bar{\Sigma}^a\tilde{H}^\dagger\sigma^a L$
$\Sigma_1$	$F(1, 3, -1)$	$\frac{1}{2}\lambda_{\Sigma_1}\bar{\Sigma}_1^a H^\dagger\sigma^a L$
$\Delta_1$	$F(1, 2, -1/2)$	$\lambda_{\Delta_1}\bar{\Delta}_1 H e$
$\Delta_3$	$F(1, 2, -3/2)$	$\lambda_{\Delta_3}\bar{\Delta}_3\tilde{H} e$
$F_4$	$F(1, 4, 1/2)$	–
$U$	$F(3, 1, 2/3)$	$\lambda_U\bar{U}\tilde{H}^\dagger Q$
$Q_5$	$F(3, 2, -5/6)$	$\lambda_{Q_5}\bar{Q}_5\tilde{H} d$
$Q_7$	$F(3, 2, 7/6)$	$\lambda_{Q_7}\bar{Q}_7 H u$
$T_1$	$F(3, 3, -1/3)$	$\frac{1}{2}\lambda_{T_1}\bar{T}_1^a H^\dagger\sigma^a Q^b$
$T_2$	$F(3, 3, 2/3)$	$\frac{1}{2}\lambda_{T_2}\bar{T}_2^a\tilde{H}^\dagger\sigma^a Q^b$
$W'_1$	$V(1, 1, 1)$	$\frac{1}{2}g_{W'_1}^{du}W_1^{\prime\mu\dagger}\bar{d}\gamma_{\mu}u + g_{W'_1}^H W_1^{\prime\mu\dagger}iD_{\mu}H^T i\sigma_2 H$
$V_3$	$V(1, 2, 3/2)$	$V_3^{\mu}\bar{e}^c\gamma_{\mu}L$
$U_1$	$V(3, 1, 2/3)$	$g_{U_1}^{ed}U_1^{\mu\dagger}\bar{e}\gamma_{\mu}d + g_{U_1}^{lq}U_1^{\mu\dagger}\bar{L}\gamma_{\mu}Q$
$\bar{V}_2$	$V(\bar{3}, 2, -1/6)$	$g_{\bar{V}_2}^{ul}\bar{V}_2^{\mu}\bar{u}^c\gamma_{\mu}L + g_{\bar{V}_2}^{dq}\bar{V}_2^{\mu}\bar{d}\gamma_{\mu}i\sigma_2 Q^c$
$U_3$	$V(3, 3, 2/3)$	$g_{U_3}U_3^{a\mu\dagger}\bar{L}\gamma_{\mu}\sigma^a Q$

**Table 2:** A full list of the heavy BSM fields that appear in UV-completions of dimension-7  $\Delta L = 2$  operators. The second column depicts the representation under the SM gauge group, where  $S$ ,  $F$ , and  $V$  denote a scalar, fermion, and vector field, respectively. The third column shows the couplings to SM fields.

operators, the Weinberg operator can be generated at tree-level if either of the type-I or type-III seesaw fields  $N$  or  $\Sigma$  are present in a given simplified model, or if the type-II seesaw field  $\Delta$  is present with both couplings to a lepton doublet pair and a Higgs pair. While a

	$\mathcal{O}_{LH}$	$\mathcal{O}_{LeHD}$	$\mathcal{O}_{\bar{e}LLLH}$	$\mathcal{O}_{\bar{d}LueH}$	$\mathcal{O}_{\bar{d}LQLH1}$	$\mathcal{O}_{\bar{d}LQLH2}$	$\mathcal{O}_{\bar{Q}uLLH}$
$S$	$\Delta, N, \Sigma$						
$\Xi$	$\Delta, \Sigma$						
$h$			$\varphi, N, \Delta_3^\dagger$			$\varphi, U, Q_5^\dagger$	
$\Delta$	$S, \Xi, \Delta, \varphi, \Theta_1, \Theta_3, \Sigma$	$\Sigma, \Delta_1^\dagger$	$\varphi, \Sigma, \Delta_3^\dagger$		$\varphi, Q_5^\dagger, T_2$		$\varphi, Q_7, T_1^\dagger$
$\varphi$	$\Delta, N, \Sigma$		$h, \Delta, N, \Sigma$		$\Delta, N, \Sigma$	$h, \Sigma$	$\Delta, N, \Sigma$
$\Theta_1$	$\Delta, \Sigma$						
$\Theta_3$	$\Delta, \Sigma_1^\dagger$						
$S_1$				$\tilde{R}_2, N, Q_5^\dagger$	$\tilde{R}_2, N, Q_5^\dagger$		
$\tilde{R}_2$				$S_1, \Delta_1^\dagger, Q_7$	$S_1, S_3, N, \Sigma, T_2$	$S_3, \Sigma, U$	
$S_3$					$\tilde{R}_2, \Sigma, Q_5^\dagger$	$\tilde{R}_2, \Sigma, Q_5^\dagger$	
$N$	$S, \varphi, \Delta_1^\dagger$	$\Delta_1^\dagger$	$h, \varphi$	$S_1, W'_1, U_1$	$\varphi, S_1, \tilde{R}_2$		$\varphi, U_1, \bar{V}_2^\dagger$
$\Sigma$	$S, \Xi, \Delta, \varphi, \Theta_1, \Delta_1^\dagger, F_4$	$\Delta, \Delta_1^\dagger$	$\Delta, \varphi$		$\varphi, \tilde{R}_2, S_3$	$\varphi, \tilde{R}_2, S_3$	$\varphi, \bar{V}_2^\dagger, U_3$
$\Sigma_1^\dagger$	$\Theta_3$						
$\Delta_1^\dagger$	$N, \Sigma$	$\Delta, N, \Sigma$		$\tilde{R}_2, W'_1, \bar{V}_2^\dagger$			
$\Delta_3^\dagger$			$h, \Delta$				
$F_4$	$\Sigma$						
$U$						$h, \tilde{R}_2$	
$Q_5^\dagger$				$S_1, V_3, \bar{V}_2^\dagger$	$\Delta, S_1, S_3$	$h, S_3$	
$Q_7$				$\tilde{R}_2, V_3, U_1$			$\Delta, U_1, U_3$
$T_1^\dagger$							$\Delta, \bar{V}_2^\dagger$
$T_2$					$\Delta, \tilde{R}_2$		
$W'_1$				$N, \Delta_1^\dagger, V_3$			
$V_3$				$Q_5^\dagger, Q_7, W'_1$			
$U_1$				$N, Q_7, \bar{V}_2^\dagger$			$N, Q_7, \bar{V}_2^\dagger$
$\bar{V}_2^\dagger$				$\Delta_1^\dagger, Q_5^\dagger, U_1$			$N, \Sigma, T_1^\dagger, U_1, U_3$
$U_3$							$\Sigma, Q_7, \bar{V}_2^\dagger$

**Table 3:** Combinations of BSM fields (c.f. Tab. 2) that realize the different dimension-7  $\Delta L = 2$  operators at tree-level. The fields to the left can be combined with either of the fields in the same row to realize the operator shown at the top of the corresponding column. Each field has its own row and appears also in the entries in other rows, such that each combination leading to a distinct simplified model is listed exactly twice.



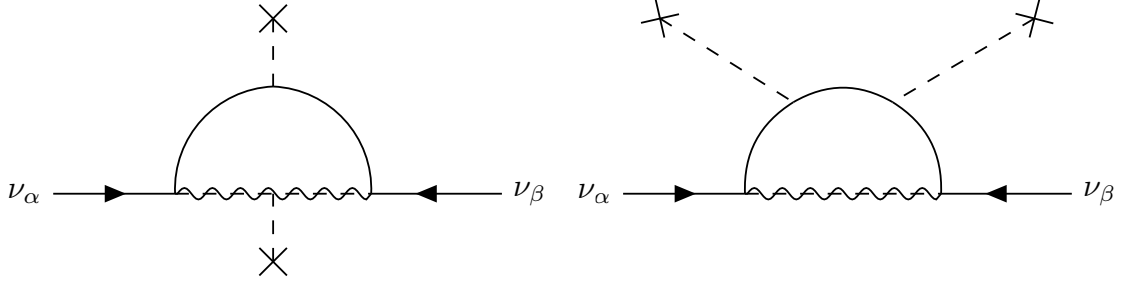


**Figure 1:** Radiative neutrino mass realised via topology I (left) and topology II (right).

UV-completion with either  $N$  or  $\Sigma$  does generate the Weinberg operator, it could be the case that their coupling to the SM is suppressed and a higher dimensional operator would dominate. However, this higher dimensional operator would be of dimension-9 and not 7. The reason for this is that any  $\Delta L = 2$  dimension-7 operator containing at least one Higgs field and two lepton doublets<sup>2</sup> can be written as  $LH \times LO^{(3)}$ , where  $O^{(3)}$  denotes a three-dimensional object. The factor  $LH$  can couple to one of the seesaw fermions  $F \in \{N, \Sigma\}$ , such that the two parts  $LH$  and  $LO^{(3)}$  of the dimension-7 operator are connected via this field. If the  $FLH$  coupling is large, it can be used twice to give a dimension-5 operator of the form  $LHLLH$ , which is exactly the Weinberg operator. We then expect this operator to dominate over the dimension-7 operator. However, if the  $FLO^{(3)}$  coupling is significantly larger, we can instead use this coupling twice to get a dimension-9 operator of the form  $LO^{(3)}LO^{(3)}$ , which should dominate over the dimension-7 operator since it does not contain the suppressed  $FLH$  coupling. In neither scenario do we have a dimension-7 operator providing the dominant contribution. As dimension-9 operators are beyond the scope of our analysis, we do not further evaluate the UV-completions containing  $N$  or  $\Sigma$  in the following sections, except simply to note down how and in which operators they appear. Note that since the type-II seesaw field  $\Delta$  couples twice to the SM, via  $\Delta HH$  and  $\Delta LL$ , it does not generate the dimension-5 operator if only one coupling constant is non-vanishing, and it can therefore participate in dominant dimension-7 operators. However, the corresponding neutrino mass diagrams are often topologically equivalent to radiative corrections of the type-II seesaw diagram.

### 3 Neutrino masses without tree-level dim-5 Weinberg operator

In this section we discuss the different neutrino mass topologies that can be generated in the tree-level UV-completions of the dimension-7  $\Delta L = 2$  operators. The operators that generate such tree-level UV-completions can be divided into three classes:  $\Psi^2 H^4$ ,  $\Psi^2 H^3 D$ , and  $\Psi^4 H$ , where  $\Psi$  denotes a fermion,  $H$  the Higgs field, and  $D$  a covariant derivative.

#### $\Psi^4 H$

Operators of type  $\Psi^4 H$  lead to two topologies for 1-loop radiative neutrino masses, as shown in Fig. 1. In topology I (Fig. 1 left), two new bosonic fields are introduced, which

<sup>2</sup>A similar argument can be made for the case where one of the lepton doublets is exchanged for a singlet.

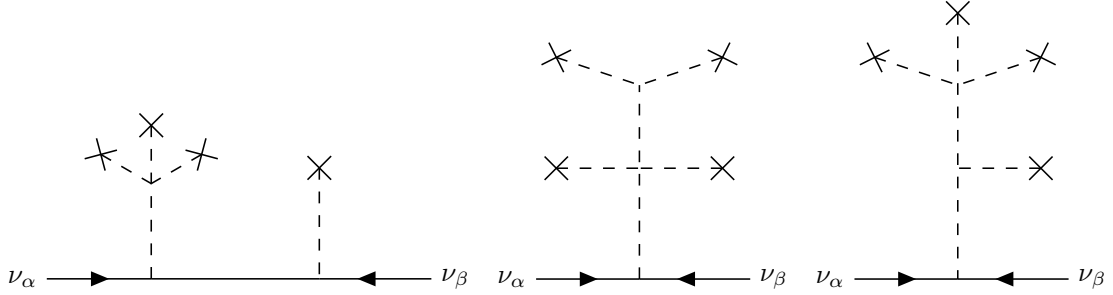


**Figure 2:** Tree-level neutrino mass realised via topology III (left), topology IV (centre) and topology V (right).

subsequently mix via a dimensionful coupling to the Higgs field. In topology II (Fig. 1 right) there is one new boson and one (vector-like) fermion. For  $N$  or  $\Sigma$  mediators there is a third topology with a Higgs vacuum expectation value (vev) insertion on a lepton leg outside the loop. Neutrino mass diagrams generated from UV-completions of operators of this type will contain at least one loop, since we need to close off two out of the four external fermion legs in order to get a self-energy type diagram for the remaining two. The bosonic mediators may be scalar or vector, depending on whether they contract a spinor with an antispinor (vector), or if they contract two spinors or antispinors (scalar). If the bosonic mediator in topology II is the type-II seesaw field  $\Delta$  there is an additional diagram for operator  $\mathcal{O}_{\bar{e}LLLH}$  where the fermion loop is disconnected from the neutrinos and the two fermion lines are coupled via  $\Delta$ . This can be seen as a vertex correction to the regular type-II seesaw diagram.

### $\Psi^2 H^3 D$

There is only a single dimension-7  $\Delta L = 2$  operator of type  $\Psi^2 H^3 D$ , namely  $\mathcal{O}_{LeHD}$ . Furthermore, this operator only has a single tree-level UV-completion which does not lead to the Weinberg operator, namely the combination of  $\Delta$  and  $\Delta_1^\dagger$  leading to topology I. Unlike the  $\Psi^4 H$ -type operators,  $\mathcal{O}_{LeHD}$  contains only one lepton doublet. In order to generate a neutrino mass, the lepton singlet must be converted into a doublet via a Higgs interaction, and this is done by closing a loop with one of the three external Higgs fields, such that there are only two insertions of the Higgs vev, and topology I is generated.

### $\Psi^2 H^4$

For type  $\Psi^2 H^4$  there is again only a single operator, namely  $\mathcal{O}_{LH}$  Refs. [14, 15]. Such a simple extension leads to a wide range of tree-level UV-completions containing either two or three new fields. For consistency with the other operators, we will here only focus on UV-completions with two fields.

$$\mathcal{O}_{LH} = \epsilon_{ij}\epsilon_{mn}(\overline{L}_p^c L_r^m) H^j H^n (H^\dagger H)$$

	$\mathcal{S}$	$\Xi$	$\Delta$	$\varphi$	$\Theta_1$	$\Theta_3$	$N$	$\Sigma$	$\Sigma_1^\dagger$	$\Delta_1^\dagger$	$F_4$
$\mathcal{S}$			IV				○	○			
$\Xi$			IV					○			
$\Delta$	IV	IV	○	V	V	V		○			
$\varphi$			V				○	○			
$\Theta_1$			V					○			
$\Theta_3$			V						III		
$N$	○			○						○	
$\Sigma$	○	○	○	○	○					○	○
$\Sigma_1^\dagger$						III					
$\Delta_1^\dagger$							○	○			
$F_4$								○			

$$\mathcal{O}_{LeHD} = \epsilon_{ij}\epsilon_{mn}(\overline{L}_p^c \gamma_\mu e_r) H^j (H^m i D^\mu H^n)$$

	$\Delta$	$N$	$\Sigma$	$\Delta_1^\dagger$
$\Delta$			○	●
$N$				○
$\Sigma$	○			○
$\Delta_1^\dagger$	●	○	○	

$$\mathcal{O}_{\bar{e}LLLH} = \epsilon_{ij}\epsilon_{mn}(\overline{e}_p L_r^i)(\overline{L}_s^c L_t^m) H^n$$

	$h$	$\Delta$	$\varphi$	$N$	$\Sigma$	$\Delta_3^\dagger$
$h$			I	○		II
$\Delta$			●		○	II
$\varphi$	I	●		○	○	
$N$	○		○			
$\Sigma$		○	○			
$\Delta_3^\dagger$	II	II				

$$\mathcal{O}_{\bar{d}LueH} = \epsilon_{ij}(\overline{d}_p L_r^i)(\overline{u}_s e_t) H^j$$

	$S_1$	$\tilde{R}_2$	$N$	$\Delta_1^\dagger$	$Q_5^\dagger$	$Q_7$	$W_1'$	$V_3$	$U_1$	$\tilde{V}_2^\dagger$
$S_1$		I*	○		II*					
$\tilde{R}_2$	I*			II*		II*				
$N$	○						○		○	
$\Delta_1^\dagger$		II*					II*			II*
$Q_5^\dagger$	II*							II*		II*
$Q_7$		II*						II*	II*	
$W_1'$			○	II*				I*		
$V_3$					II*	II*	I*			
$U_1$			○			II*				I*
$\tilde{V}_2^\dagger$				II*	II*					I*

$$\mathcal{O}_{\bar{d}LQLH1} = \epsilon_{ij}\epsilon_{mn}(\overline{d}_p L_r^i)(\overline{Q}_s^c L_t^m) H^n$$

	$\Delta$	$\varphi$	$S_1$	$\tilde{R}_2$	$S_3$	$N$	$\Sigma$	$Q_5^\dagger$	$T_2$
$\Delta$		●						●	●
$\varphi$	●					○	○		
$S_1$				I		○		II	
$\tilde{R}_2$			I		I	○	○		II
$S_3$				I			○	II	
$N$		○	○	○					
$\Sigma$		○		○	○				
$Q_5^\dagger$	●		II		II				
$T_2$	●			II					

$$\mathcal{O}_{\bar{d}LQLH2} = \epsilon_{im}\epsilon_{jn}(\overline{d}_p L_r^i)(\overline{Q}_s^c L_t^m) H^n$$

	$h$	$\varphi$	$\tilde{R}_2$	$S_3$	$\Sigma$	$U$	$Q_5^\dagger$
$h$		I*				II*	II*
$\varphi$	I*				○		
$\tilde{R}_2$				I*	○	II*	
$S_3$			I*		○		II*
$\Sigma$		○	○	○			
$U$	II*		II*				
$Q_5^\dagger$	II*			II*			

$$\mathcal{O}_{\bar{Q}uLLH} = \epsilon_{ij}(\overline{Q}_p u_r)(\overline{L}_s^c L_t^i) H^j$$

	$\Delta$	$\varphi$	$N$	$\Sigma$	$Q_7$	$T_1^\dagger$	$U_1$	$\tilde{V}_2^\dagger$	$U_3$
$\Delta$		●			●	●			
$\varphi$	●		○	○					
$N$		○					○	○	
$\Sigma$		○						○	○
$Q_7$	●						II		II
$T_1^\dagger$	●							II	
$U_1$			○		II			I	
$\tilde{V}_2^\dagger$			○	○		II	I		I
$U_3$				○	II			I	

**Table 4:** Tree-level UV-completions of dimension-7  $\Delta L = 2$  operators. A Roman number denotes the topology, where an asterisk indicates a two-loop diagram obtained by an additional  $W$ -boson loop. An empty (filled) circle indicates the Weinberg operator (radiative correction to the type-II seesaw diagram).

In Tab. 4 the combinations of BSM fields that lead to tree-level UV-completions of the  $\Delta L = 2$  dimension-7 SMEFT operators are shown for one operator at a time, along with the corresponding radiative neutrino mass topology. A Roman number in a given entry of these tables indicate that the corresponding neutrino mass topology shown in Fig. 1 or 2 is generated by the combination of the two fields at the left and top that have an overlapping row and column at this entry. Entries with an asterisk indicate that a two-loop diagram can be generated using the one-loop topology with the addition of an  $H$ -loop or a  $W$ -loop, such that the neutrino mass is generated at 2-loop order. An empty circle denotes that the dimension-5 operator is generated via the type-I or type-III seesaw, and a filled circle indicates that the corresponding neutrino mass diagram is topologically equivalent to a loop correction to the type-II seesaw diagram.

## 4 Loop neutrino masses: cut-off EFT estimates vs. exact UV results

### 4.1 Single-scale EFT estimate based on cutoff regularisation

In principle, any  $\Delta L = 2$  SMEFT operator can lead to Majorana neutrino masses. For dimension-7 operators with four fermions to generate neutrino masses, two fermion legs have to be closed into a loop, leading to an additional Yukawa coupling. For operators with external lepton singlets, an additional charged Higgs interaction may be needed to convert it into a lepton doublet, and external charged leptons belonging to a doublet can be converted to neutrinos via additional  $W$  interactions. In Refs. [25, 29, 30] and related literature, the contributions of higher-dimensional effective interactions to neutrinos mass via such loop diagrams have been estimated using a cut-off approximation, in which the theory is characterized by a single cut-off scale  $\Lambda$ . In this approach, momentum integrals are then limited by this cut-off, with NP emerging above  $\Lambda$  to regularize the theory. Power counting of momentum factors can determine these divergences, but loop integrals can become complex, particularly due to momentum factors in Dirac propagators, which must appear in pairs to contribute to UV divergences. As stated in Ref. [25], when adding loops to induce power-law divergences proportional to  $\Lambda$ , the process should be limited to the point where the suppression of the induced term is no worse than  $1/\Lambda$ . Beyond this, additional divergences only provide small finite corrections that renormalise lower-order terms.

As further stated in Ref. [25], each loop comes with a numerical suppression factor due to the normalization of the loop four-momentum integrals, specifically a factor of  $1/(16\pi^2)$ . This suppression offsets enhancements from divergence factors. Quadratically divergent loop diagrams are often proportional to the lowest-order contribution, multiplied by factors depending on the number of loops and  $\Lambda/v$ , where  $v$  is the Higgs vev. For diagrams to dominate over leading-order contributions,  $\Lambda$  must be generally greater than about 2 TeV (for a discussion see Ref. [30]). However, many loop diagrams are logarithmically divergent or even convergent, making the enhancement of LNV rates inefficient at the low scales accessible to future experiments.

With all these considerations and caveats, the expressions for neutrino masses shown in the third column of Tab. 5 can be obtained. Below we will present an alternative to this

$\mathcal{O}$	Operator	EFT Neutrino mass
$\mathcal{O}_{LH}^{pr}$	$\epsilon_{ij}\epsilon_{mn}(\overline{L}_p^c L_r^m)H^j H^n (H^\dagger H)$	$(\frac{1}{16\pi^2} + \frac{v^2}{\Lambda^2})\frac{v^2}{\Lambda}$
$\mathcal{O}_{LeHD}^{pr}$	$\epsilon_{ij}\epsilon_{mn}(\overline{L}_p^c \gamma_\mu e_r)H^j (H^m i D^\mu H^n)$	$y_e^{ri} \frac{g'}{(16\pi^2)^2} \frac{v^2}{\Lambda}$
$\mathcal{O}_{\bar{e}LLLH}^{prst}$	$\epsilon_{ij}\epsilon_{mn}(\overline{e}_p L_r^i)(\overline{L}_s^c L_t^m)H^n$	$(y_e^{pr} + y_e^{ps} + y_e^{pt})\frac{1}{16\pi^2}\frac{v^2}{\Lambda}$
$\mathcal{O}_{\bar{d}LueH}^{prst}$	$\epsilon_{ij}(\overline{d}_p L_r^i)(\overline{u}_s^c e_t)H^j$	$\sum_{ij} y_u^{sj} y_d^{jp} y_e^{ti} \frac{1}{(16\pi^2)^2} \frac{v^2}{\Lambda}$
$\mathcal{O}_{\bar{d}LQLH1}^{prst}$	$\epsilon_{ij}\epsilon_{mn}(\overline{d}_p L_r^i)(\overline{Q}_s^c L_t^m)H^n$	$y_d^{ps} \frac{1}{16\pi^2} \frac{v^2}{\Lambda}$
$\mathcal{O}_{\bar{d}LQLH2}^{prst}$	$\epsilon_{im}\epsilon_{jn}(\overline{d}_p L_r^i)(\overline{Q}_s^c L_t^m)H^n$	$y_d^{ps} \frac{g^2}{(16\pi^2)^2} \frac{v^2}{\Lambda}$
$\mathcal{O}_{\overline{Q}uLLH}^{prst}$	$\epsilon_{ij}(\overline{Q}_p u_r)(\overline{L}_s^c L_t^i)H^j$	$y_u^{pr} \frac{1}{16\pi^2} \frac{v^2}{\Lambda}$

**Table 5:** List of the  $\Delta L = 2$  dimension-7 operators that appear in Tabs. 4, along with the cut-off expression for the neutrino mass [25].

prescription that, as will be argued, better matches the results stemming from the UV-complete scenarios.

## 4.2 An explicit UV model example and exact loop computation

In this section we provide a more in-depth analysis into one of the simplified models as an example. This model consists of an extension to the SM with two scalar leptoquarks,  $\tilde{R}_2$  and  $S_1$ . The Lagrangian is given by [31–33]

$$\begin{aligned} \mathcal{L} = & \mathcal{L}_{\text{SM}} - \tilde{R}_2^\dagger(\square + m_{\tilde{R}_2}^2)\tilde{R}_2 - S_1^*(\square + m_{S_1}^2)S_1 + \mu S_1 H^\dagger \tilde{R}_2 \\ & - g_1^{ij} \overline{L}_i i \sigma_2 \tilde{R}_2^* \overline{d}_j^c - g_2^{ij} Q_i \epsilon L_j S_1 - g_3^{ij} \overline{u}_i^c e_j S_1 + \text{h.c.}, \end{aligned} \quad (4.1)$$

where  $\square = \eta^{\mu\nu} \partial_\mu \partial_\nu$  is the d'Alembert operator,  $i, j, k$  are flavour indices, and  $\epsilon$  denotes that the  $SU(2)_L$  indices of the two doublets of this term should be contracted via the antisymmetric Levi-Civita tensor. If both  $\tilde{R}_2$  and  $S_1$  are heavy with respect to the electroweak symmetry breaking scale, Eq. (4.1) leads to the generation of operator  $\mathcal{O}_{\bar{d}LQLH1}$  and  $\mathcal{O}_{\bar{d}LueH}$  at the low scale, with corresponding Wilson coefficients

$$C_{\bar{d}LQLH1}^{ijkn} = -\frac{\mu g_1^{ni} g_2^{kj}}{m_{\tilde{R}_2}^2 m_{S_1}^2}, \quad C_{\bar{d}LueH}^{ijkn} = \frac{\mu g_1^{ji} g_3^{kn}}{m_{\tilde{R}_2}^2 m_{S_1}^2}. \quad (4.2)$$

In Fig. 3 (left column) we show how these operators are generated in this model. This operator can then lead to  $0\nu\beta\beta$  decay and LNV rare kaon decays [34–36].

This model also leads to radiative neutrino masses [24, 31–33, 35–40] as well as leptogenesis [40]. At lowest order we have a 1-loop neutrino mass shown in Fig. 3 (top right). If the coupling  $g_2$  is suppressed, neutrino masses can still be generated at 2-loop order via  $g_3$  as shown in Fig. 3 (bottom right), corresponding to the set of couplings that generate

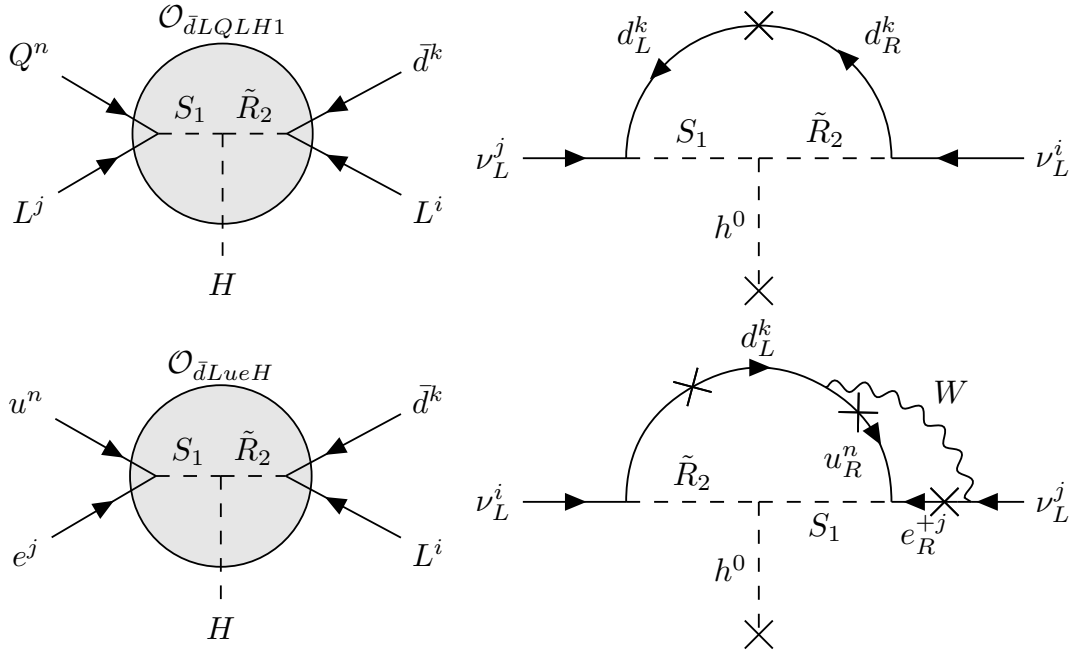


**Figure 3:** **Left column:** Operators  $\mathcal{O}_{\bar{d}LQLH1}$  (top) and  $\mathcal{O}_{\bar{d}LueH}$  (bottom) generated by the model described in the text. **Right column:** Radiative neutrino mass diagrams generated in the model described in the text, corresponding to the set of coupling constants that lead to  $\mathcal{O}_{\bar{d}LQLH1}$  (top) and  $\mathcal{O}_{\bar{d}LueH}$  (bottom).

$\mathcal{O}_{\bar{d}LueH}$ . The mass matrix for the leptoquark pair is given by

$$M^2 = \begin{pmatrix} m_{\tilde{R}_2}^2 & \mu v \\ \mu v & m_{S_1}^2 \end{pmatrix}. \quad (4.3)$$

Diagonalising this matrix leads to two mass eigenstates  $m_{LQ_{1,2}}$  given by

$$m_{LQ_{1,2}}^2 = \frac{1}{2} \left( m_{\tilde{R}_2}^2 + m_{S_1}^2 \mp \sqrt{(m_{\tilde{R}_2}^2 - m_{S_1}^2)^2 + \mu^2 v^2} \right). \quad (4.4)$$

Using these mass eigenstates we can express the 1-loop neutrino mass from Fig. 3 (top right) as [24]

$$(m_\nu)_{ij} = \sum_k \frac{3 \sin(2\theta) y_{kk}^d v g_1^{ik} g_2^{kj}}{32\pi^2} \log \frac{m_{LQ_2}^2}{m_{LQ_1}^2}, \quad (4.5)$$

where  $y^d$  is the SM down-type quark Yukawa coupling matrix. The mixing angle  $\theta$  is given by [31, 32, 41]

$$\tan(2\theta) = \frac{2\mu v}{m_{\tilde{R}_2}^2 - m_{S_1}^2}, \quad (4.6)$$

where  $V$  is the CKM matrix. The 2-loop radiative neutrino mass shown in Fig. 3 (bottom

right) can be expressed as [41]

$$(m_\nu)_{ij} = \frac{3 \sin(2\theta) v^3 g^2}{(16\pi^2)^2 m_{LQ_1}^2} \left( g_1^{ik} y_{kk}^d V_{kl}^T y_{ll}^u (g_2)^{lj} y_{jj}^e + y_{ii}^e (g_2^T)^{il} y_{ll}^u V_{lk} y_{kk}^d (g_1^T)^{kj} \right) \times I_{jkl}(m_{LQ_1}^2, m_{LQ_2}^2, m_W^2), \quad (4.7)$$

where for massless SM fermions, the function  $I_{jkl}(m_{LQ_1}^2, m_{LQ_2}^2, m_W^2)$  simplifies to [41]

$$I(m_{LQ_1}^2, m_{LQ_2}^2, m_W^2) \approx \left( 1 - \frac{m_{LQ_1}^2}{m_{LQ_2}^2} \right) \times \left[ 1 + \frac{\pi^2}{3} + \frac{m_{LQ_1}^2 \log \frac{m_{LQ_2}^2}{m_W^2} - m_{LQ_2}^2 \log \frac{m_{LQ_1}^2}{m_W^2}}{m_{LQ_1}^2 - m_{LQ_2}^2} + \frac{1}{2} \frac{m_{LQ_1}^2 \log^2 \frac{m_{LQ_2}^2}{m_W^2} - m_{LQ_2}^2 \log^2 \frac{m_{LQ_1}^2}{m_W^2}}{m_{LQ_1}^2 - m_{LQ_2}^2} \right]. \quad (4.8)$$

Below we compare the 1- and 2-loop neutrino mass expressions in this model, given by Eqs. (4.5) and (4.7), with the cut-off-regularisation-based estimates in Tab. 5. The cut-off-regularisation-based one-loop neutrino mass estimate for  $\mathcal{O}_{\bar{d}LQLH1}$  in the EFT shown in Tab. 5 can be expressed in the flavour basis as

$$(m_\nu)_{ij} = \frac{y_{nk}^d}{16\pi^2} \frac{v^2}{\left( C_{\bar{d}LQLH1}^{kinj} \right)^{-1/3}}, \quad (4.9)$$

which should be compared against the exact model result Eq. (4.5). Similarly, the two-loop neutrino mass estimate for  $\mathcal{O}_{\bar{d}LueH}$  in the cut-off regularisation can be expressed as

$$(m_\nu)_{ij} = g^2 y_{sl}^u V_{lr} y_{rp}^d y_{jk}^e \frac{1}{(16\pi^2)^2} \frac{v^2}{\left( C_{\bar{d}LueH}^{pisk} \right)^{-1/3}}, \quad (4.10)$$

which should be compared against the exact model result Eq. (4.7).

Comparing the exact loop results with the cut-off regularisation, we notice that the exact results are sensitive to the hierarchy of scales between the two heavy fields. We can vary the ratio between  $m_{\tilde{R}_2}$  and  $m_{S_1}$  to show the dependence of the neutrino mass on the hierarchy of scales between the two heavy fields. To do this we define the hierarchy parameter  $\xi$  as

$$\xi \equiv \frac{\max(m_{\Phi_1}, m_{\Phi_2})}{\min(m_{\Phi_1}, m_{\Phi_2})}, \quad (4.11)$$

where in this model we have  $\Phi_1 \rightarrow \tilde{R}_2$  and  $\Phi_2 \rightarrow S_1$ . In Fig. 4 we compare the different neutrino mass expressions for the benchmark points described above with  $m_{\tilde{R}_2} > m_{S_1}$  at both 1- and 2-loop. We assume normal ordering and  $CP$  conservation in the neutrino sector, and use the neutrino mixing angles given by NUFIT v6.0 [42], explicitly  $\theta_{12} = 33.68^\circ$ ,

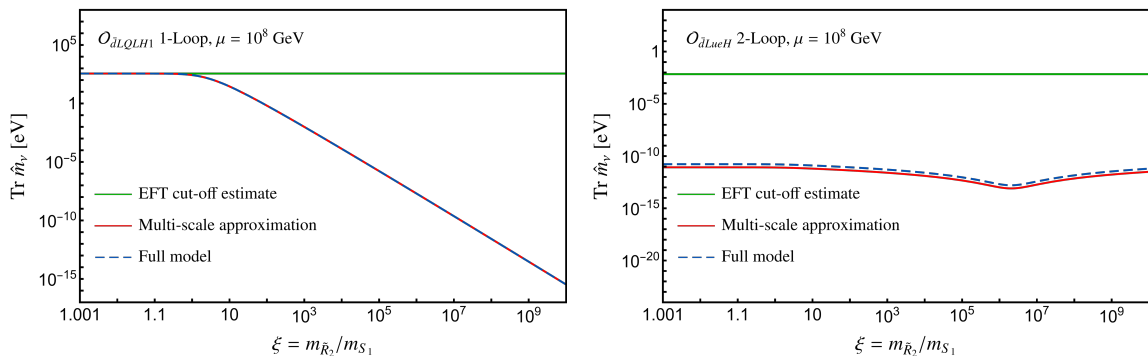


**Figure 4:** The sum of neutrino masses as a function of the degree of hierarchy between  $m_{\tilde{R}_2}$  and  $m_{S_1}$ , assuming  $m_{\tilde{R}_2} > m_{S_1}$ , as quantified by the parameter  $\xi$ , at 1-loop (left) and 2-loop (right) using  $\mu = 10^8$  GeV. The green line shows the cut-off estimate from Eq. (4.9), the blue line shows the full model-based expression from Eqs. (4.5) (1-loop) and (4.7) (2-loop). The red line shows the expression obtained in the simplified model estimate.

$\theta_{23} = 44.3^\circ$ , and  $\theta_{13} = 8.56^\circ$ .

For the 1-loop mass, we see that the expressions agree quite well for small  $\xi$ , i.e. when there is a small mass difference between  $m_{\tilde{R}_2}$  and  $m_{S_1}$ . For larger  $\xi$  the neutrino mass is smaller in the exact model-based expression, while remaining constant in the cut-off estimate, leading to an over-estimation of the constraint on the Wilson coefficient coming from neutrino masses. Comparing with the leptoquark model expressions we see that capturing the effect of a sizable hierarchy in the internal degrees of freedom of an operator is crucial for determining the available region of parameter space correctly.

Cut-off estimates of the neutrino mass, such as the expression given in the third column of Tab. 5, have been commonly used in the literature to estimate the constraint of small neutrino masses on higher-dimensional  $\Delta L = 2$  operators. In this section we have shown that such estimates fail to capture the effect of a non-vanishing hierarchy in the internal degrees of freedom. As can be seen in Fig. 4, such a hierarchy can relax the neutrino mass constraint by many orders of magnitude.

## 5 A simplified multi-scale approach to loop neutrino masses

It is well known that a much more robust approach compared to that of based on cut-off regularisation is provided by the renormalization group (RG) improved perturbation theory [43]. However, the derivation and implementation of the full RG equations order by order for an independent basis of higher dimensional operators is often quite cumbersome. For instance, recently in Refs. [44, 45] the RG equations for dimension-7 LNV operators at one-loop order has been derived. In Ref. [21] a leading-log approximation for light neutrino masses arising from LNV operators up to dimension-7 was presented, keeping only the largest SM Yukawa couplings. A detailed technical treatment of the full RG equations is beyond the scope of this work. Instead, in what follows, we will discuss the limitations of the cut-off based approach which leads to a poor approximation when the



heavy new physics degrees of freedom generating radiative neutrino masses are hierarchical in mass. We will show that a simple dimensional regularisation based approach combined with simple scaling arguments can approximate the loop neutrino masses arising from higher dimensional operators much more accurately compared to the cut-off based approach. This simplified multi-scale formalism gives a quick way to accurately estimate the loop neutrino masses using simple momentum expansion arguments without a full implementation of the full set of RGE equations, which can often be a very cumbersome exercise.

To highlight the limitation of the cut-off regularisation approach let us consider the simple toy Lagrangian

$$\mathcal{L}^{\text{full}} = \int d^4x \left\{ -\frac{1}{2} \partial_\mu \Phi \partial^\mu \Phi - \frac{1}{2} M^2 \Phi^2 + \bar{\psi} (i\gamma^\mu \partial_\mu - m) \psi + iY \Phi \bar{\psi} \gamma^5 \psi - \frac{1}{4!} \lambda \Phi^4 \right\}, \quad (5.1)$$

where  $\Phi$  with mass  $M$  is a heavy pseudo-scalar and  $\psi$  is a light fermion with mass  $m$ , such that  $M \gg m$ . If the typical energy scale of an observable  $E$  is such that  $m \leq E \ll M$ , then a two-point one-loop fermionic tadpole correction in the EFT obtained after integrating out the heavy scalar  $\Phi$  is given by

$$G_2^{\text{EFT}} = -\frac{Y^2 m}{M^2} \int \frac{d^4k}{(2\pi)^4} \frac{1}{k^2 + m^2 - i\epsilon} = -\frac{m}{\Lambda^2} \int \frac{d^4k}{(2\pi)^4} \frac{1}{k^2 + m^2 - i\epsilon}, \quad (5.2)$$

where to write the last equality we have used the definition that the EFT scale  $\Lambda \equiv M/Y$ . According to the cut-off-regularisation-based approach mentioned above, one would cut off the integral over  $k$  at the heavy scale  $\Lambda$ , since the EFT obtained by integrating out  $\Phi$  is expected to be valid at energies  $E < \Lambda$  [46]. This leads to a resulting factor of  $\Lambda^2$  in the numerator which would cancel against the  $1/\Lambda^2$  in the Wilson coefficient, giving a result that is independent of the heavy UV scale  $\Lambda$ . This is of course not consistent with the power counting rule suggesting a dependence  $E^2/\Lambda^2$ .

Using a dimensional regularisation approach instead, the integral is generalised to  $d = 4 - \epsilon$  dimensions, where  $\epsilon$  denotes the deviation from  $d = 4$ . Then the integral in Eq. (5.2) can be expressed in the form

$$G_{2,\text{dim-reg}}^{\text{EFT}} = -\frac{\tilde{\mu}_r^\epsilon m}{\Lambda^2} \int \frac{d^{4-\epsilon}k}{(2\pi)^{4-\epsilon}} \frac{1}{k^2 + m^2 - i\epsilon} = \frac{i}{16\pi^2} \frac{m^3}{\Lambda^2} \left[ \frac{2}{\epsilon} + 1 + \log \left( \frac{\mu_r^2}{m^2} \right) + \mathcal{O}(\epsilon) \right], \quad (5.3)$$

where the renormalisation scale  $\tilde{\mu}_r$  replaces  $Y \rightarrow Y \tilde{\mu}_r^{\epsilon/2}$  to ensure that  $Y$  is dimensionless, and where  $\mu_r$  is given by  $\mu_r = \sqrt{4\pi} e^{-\gamma} \tilde{\mu}_r$ , with  $\gamma$  being the Euler constant. The UV-divergent piece proportional to  $1/\epsilon$  drops out in the  $\overline{\text{MS}}$ -scheme and we obtain a loop integral result which is now consistent with the power-counting expectation.

While the EFT result in Eq. (5.3) can be recovered by evaluating the integral in the full theory, c.f. Eq. (5.1), using dimensional regularisation and then expanding in the heavy mass scale  $M$ , it is well known that the loop integral and the series expansion does not commute in general [43]. This leads to a difference in the exact theory vs. the EFT estimation of loops. This difference is analytic in the IR scale  $m$  and leads to a matching contribution,

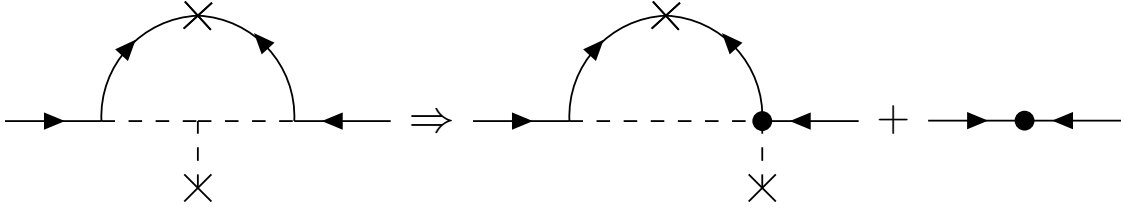


**Figure 5:** One-loop neutrino mass diagrams in the full and effective theories. The crosses represent fermion mass insertions and the thick circle represents contact interactions.

which needs to be added to the EFT result to correctly reproduce the full theory result. To be more concrete, the full theory computation differs from the result in Eq. (5.3) by terms proportional to  $\log(M^2/\mu_r^2)$  at one-loop order and by higher powers of the same log for higher order loops [43].

A particularly interesting scenario is when two largely different heavy NP scales are present in the full theory  $M \gg m \gg E$ , where  $E$  is the energy scale of the experimental observable we are interested in. In the presence of a large hierarchy between different scales  $M$  and  $m$  in the full theory, the relatively large logs appearing in the loop integrals of the form  $\log(m^2/M^2)$  can be split into two contributions of the form  $\log(M^2/m^2) = \log(M^2/\mu_r^2) - \log(m^2/\mu_r^2)$ . The first part can be absorbed in the Wilson coefficient (upon integrating out the large scale  $M$ ) by choosing the renormalisation scale  $\mu_r = M$  and doing the matching procedure at  $\mu_r = M$ . The second part, on the other hand, can be obtained by calculating the one-loop corrections in the EFT at  $\mu_r = m$ , which can be done using the RG equations capturing the running of the Wilson coefficients from  $\mu_r = M$  to  $\mu_r = m$ . We note that the EFT after integrating out  $M$  depends on either ratios of the form  $(m^2/M^2)$  or  $\log(M^2/\mu_r^2)$ . If we evaluate the Wilson coefficient at  $\mu_r = M$  then the terms proportional to  $\log(M^2/\mu_r^2)$  vanish and only terms proportional to powers of  $(m^2/M^2)$  survive.

### 5.1 Simplified multi-scale formalism for one-loop neutrino masses

With the above prescription in mind, let us now consider the one-loop neutrino mass in the model example discussed in section 4.2, c.f. the top diagram in Fig. 3. We are interested in the case where the heavy new physics is hierarchical in mass. Let us consider for example the scenario where  $m_{\tilde{R}_2} \gg m_{S_1}$ . The one-loop neutrino mass diagram in the UV model and how it matches into the EFT obtained after integrating out the heaviest degree of freedom  $\tilde{R}_2$  are shown in Fig. 5, where the last diagram to the right symbolizes any potential additional effective contributions arising from integrating out the heaviest degree of freedom.

In the full theory the one-loop neutrino mass diagram in dimensional regularisation gives the integral

$$I_1 = c_m \mu_r^{2\epsilon} \int \frac{d^d k}{(2\pi)^d} \frac{1}{k^2} \frac{1}{k^2 - m_{S_1}^2} \frac{1}{k^2 - m_{\tilde{R}_2}^2}, \quad (5.4)$$

where the dimensionful prefactor is given by  $c_m = g_1 g_2 v \mu m_d^2$  and we neglect the light down-type quark masses in the denominators for simplicity. Now the neutrino mass in the intermediate EFT (I-EFT) obtained after integrating out the heaviest degree of freedom

$\tilde{R}_2$  can be obtained by expanding out the above integral in the heavy mass  $m_{\tilde{R}_2}$

$$I_1^{\text{I-EFT}} = c_m \mu_r^{2\varepsilon} \int \frac{d^d k}{(2\pi)^d} \frac{1}{k^2} \frac{1}{k^2 - m_{S_1}^2} \left[ -\frac{1}{m_{\tilde{R}_2}^2} \left( 1 + \frac{k^2}{m_{\tilde{R}_2}^2} + \frac{k^4}{m_{\tilde{R}_2}^4} + \dots \right) \right]. \quad (5.5)$$

In Fig. 5, this corresponds to the left diagram of the EFT case, while there is no tree-level effective contribution in this case. Integrating term by term yields

$$\begin{aligned} I_1^{\text{I-EFT}} &= -c_m \frac{i}{16\pi^2} \frac{1}{m_{\tilde{R}_2}^2} \left[ \left( 1 + \log \left( \frac{\mu_r^2}{m_{S_1}^2} \right) \right) + \frac{m_{S_1}^2}{m_{\tilde{R}_2}^2} \left( 1 + \log \left( \frac{\mu_r^2}{m_{S_1}^2} \right) \right) \right. \\ &\quad \left. + \frac{m_{S_1}^4}{m_{\tilde{R}_2}^4} \left( 1 + \log \left( \frac{\mu_r^2}{m_{S_1}^2} \right) \right) + \dots \right] \\ &\approx -c_m \frac{i}{16\pi^2} \frac{1}{(m_{\tilde{R}_2}^2 - m_{S_1}^2)} \left[ 1 + \log \left( \frac{\mu_r^2}{m_{S_1}^2} \right) \right]. \end{aligned} \quad (5.6)$$

Now the analytic contributions  $I_1^{\text{ana}}$  missed in the EFT expansion (containing terms proportional to  $\log m_{\tilde{R}_2}$ ) can be obtained by performing an expansion of  $I_1$  and  $I_1^{\text{I-EFT}}$  in  $m_{S_1}$  and taking  $I_1^{\text{ana}} = I_{1\text{exp}} - I_{1\text{exp}}^{\text{I-EFT}}$  where the subscript ‘‘exp’’ denotes an expansion in the lighter scale  $m_{S_1}$ . The expansions  $I_{1\text{exp}}$  and  $I_{1\text{exp}}^{\text{EFT}}$  are given by

$$I_{1\text{exp}} = c_m \mu_r^{2\varepsilon} \int \frac{d^d k}{(2\pi)^d} \frac{1}{k^2} \frac{1}{k^2 - m_{\tilde{R}_2}^2} \left[ \frac{1}{k^2} \left( 1 + \frac{m_{S_1}^2}{k^2} + \frac{m_{S_1}^4}{k^4} + \dots \right) \right], \quad (5.7)$$

and

$$I_{1\text{exp}}^{\text{I-EFT}} = c_m \mu_r^{2\varepsilon} \int \frac{d^d k}{(2\pi)^d} \frac{1}{k^2} \left[ \frac{1}{k^2} \left( 1 + \frac{m_{S_1}^2}{k^2} + \frac{m_{S_1}^4}{k^4} + \dots \right) \right] \left[ -\frac{1}{m_{\tilde{R}_2}^2} \left( 1 + \frac{k^2}{m_{\tilde{R}_2}^2} + \dots \right) \right]. \quad (5.8)$$

Upon integrating term by term  $I_{1\text{exp}}^{\text{I-EFT}}$  vanishes, while  $I_{1\text{exp}}$  gives rise to a non-vanishing contribution for  $I_1^{\text{ana}}$

$$\begin{aligned} I_1^{\text{ana}} &= c_m \frac{i}{16\pi^2} \left[ \frac{1}{m_{\tilde{R}_2}^2} \left( 1 + \log \left( \frac{\mu_r^2}{m_{\tilde{R}_2}^2} \right) \right) + \frac{m_{S_1}^2}{m_{\tilde{R}_2}^4} \left( 1 + \log \left( \frac{\mu_r^2}{m_{\tilde{R}_2}^2} \right) \right) + \dots \right] \\ &\approx c_m \frac{i}{16\pi^2} \frac{1}{(m_{\tilde{R}_2}^2 - m_{S_1}^2)} \left[ 1 + \log \left( \frac{\mu_r^2}{m_{\tilde{R}_2}^2} \right) \right]. \end{aligned} \quad (5.9)$$

The whole contribution to the one-loop neutrino mass is then given by

$$\begin{aligned} I_{1\text{MS}}^{\text{total}} &= I_1^{\text{EFT}} + I_1^{\text{ana}} \\ &\approx c_m \frac{i}{16\pi^2} \frac{1}{(m_{\tilde{R}_2}^2 - m_{S_1}^2)} \log \left( \frac{m_{S_1}^2}{m_{\tilde{R}_2}^2} \right), \end{aligned} \quad (5.10)$$

where we use the subscript MS to denote that this is the result using the multi-scale

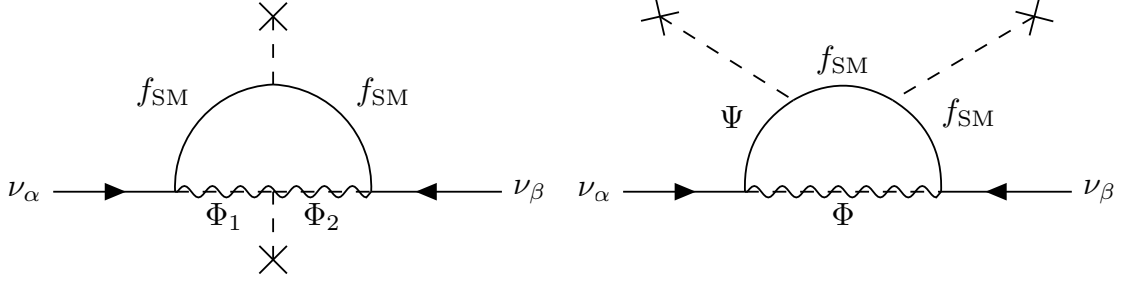


**Figure 6:** One-loop neutrino masses based on the simplified interactions in Eq. 5.19 leading to topology I (left) and Eq. 5.20 leading to topology II.

approach.

The exact expression for the loop diagram in the full model, c.f. Eq. (4.5), when expanded in the heavy scale, yields the same expression. Therefore, the above prescription represents a consistent approach to estimate the loop neutrino masses starting from an EFT interaction and without the knowledge of the exact computation in the full theory. In essence, we have split the original one-loop computation involving two hierarchical new physics scales into a two-scale EFT problem. In the particular case when  $m_{\tilde{R}_2} \rightarrow m_{S_1}$ , the above expression in the dimensional regularisation reduces to the standard single scale EFT result using cut-off regularisation, leading to a  $1/\Lambda$  dependence with  $\Lambda \sim m_{\tilde{R}_2} \sim m_{S_1}$ , c.f. Tab. 5.

## 5.2 Simplified multi-scale formalism for two-loop neutrino masses

A similar prescription can also be applied to higher loop order. However, the evaluation of the multi-loop integrals become quickly nontrivial and a number of simplifying physical assumptions can help in getting relatively simpler analytic results. Let us consider the two-loop neutrino mass diagram in the model example discussed in section 4.2, c.f. the bottom diagram in Fig. 3. To estimate the contribution using our prescription it suffices to approximate the  $W$ -boson propagator by a scalar propagator of similar mass. The complete contribution involves additional terms which are suppressed by  $m_W^2/m_{\tilde{R}_2}^2$  and  $m_W^2/m_{S_1}^2$ , which will provide subdominant corrections. Under the above approximations the two-loop neutrino mass diagram can be approximated as

$$M_\nu \simeq c'_m \int d^4 p \int d^4 q \frac{1}{p^2} \frac{1}{q^2} \frac{1}{q^2 - m_W^2} \frac{1}{(p-q)^2 - m_u^2} \frac{1}{p^2 - m_{S_1}^2} \frac{1}{p^2 - m_{\tilde{R}_2}^2} \equiv c'_m I_2, \quad (5.11)$$

where  $c'_m \sim \frac{N_c}{(2\pi)^8} m_d m_u m_e (\mu v) g^2 y_{S_1} y_{\tilde{R}_2}$ , with the  $y$ 's denoting the relevant Yukawa interactions of the leptoquarks with the SM fermions,  $N_c$  denoting the color factor, and  $\mu$  denotes the trilinear scalar coupling with mass dimension one. In the above we have ignored the flavor structure of the light new physics, which can be straightforwardly included as necessary. We have further assumed the limit of vanishing lepton- and down-type quark mass inside the loop integral. However, we note that the overall neutrino mass contribution is proportional to a prefactor containing these masses. Consequently, they cannot be taken to

be vanishing in the full expression of neutrino mass. The integral  $I$  can then be expressed in terms of the rescaled dimensionless momenta as

$$I_2 = \frac{1}{m_u^4} \int d^4 p \int d^4 q \frac{1}{p^2 q^2} \frac{1}{q^2 - r} \frac{1}{(p - q)^2 - 1} \frac{1}{p^2 - t_1} \frac{1}{p^2 - t_2}, \quad (5.12)$$

where  $r = m_W^2/m_u^2$ ,  $t_1 = m_{S_1}^2/m_u^2$  and  $t_2 = m_{\tilde{R}_2}^2/m_u^2$ . Now one can follow the same prescription as in the one-loop case. Assuming again that  $\tilde{R}_2$  is much heavier than the momentum and  $m_{S_1}$ , we can expand the corresponding propagator to obtain in the I-EFT limit

$$I_2^{\text{I-EFT}} = \frac{1}{m_u^4} \int d^4 p \int d^4 q \frac{1}{p^2 q^2} \frac{1}{q^2 - r} \frac{1}{(p - q)^2 - 1} \frac{1}{p^2 - t_1} \left[ -\frac{1}{t_2} \left( 1 + \frac{p^2}{t_2} + \frac{p^4}{t_2^2} + \dots \right) \right]. \quad (5.13)$$

Similarly, we can also use the same momentum expansion scheme as in the one-loop case to obtain the analytic contributions using

$$I_{2\text{exp}} = \frac{1}{m_u^4} \int d^4 p \int d^4 q \frac{1}{p^2 q^2} \frac{1}{q^2 - r} \frac{1}{(p - q)^2 - 1} \left[ \frac{1}{p^2} \left( 1 + \frac{t_1}{p^4} + \frac{t_1^2}{p^8} + \dots \right) \right] \frac{1}{p^2 - t_2}, \quad (5.14)$$

and

$$I_{2\text{exp}}^{\text{I-EFT}} = \frac{1}{m_u^4} \int d^4 p \int d^4 q \frac{1}{p^2 q^2} \frac{1}{q^2 - r} \frac{1}{(p - q)^2 - 1} \times \left[ \frac{1}{p^2} \left( 1 + \frac{t_1}{p^2} + \frac{t_1^2}{p^4} + \dots \right) \right] \left[ -\frac{1}{t_2} \left( 1 + \frac{p^2}{t_2} + \frac{p^4}{t_2^2} + \dots \right) \right]. \quad (5.15)$$

Now combining the leading order terms in the expansions of Eqs.(5.13), (5.14) and (5.15), we find

$$I_{2\text{MS}}^{\text{leading}} = \frac{1}{m_u^2 m_{\tilde{R}_2}^2} [-J(r, t_1) + J(r, t_2)] \quad (5.16)$$

where

$$J(r, t) = \int d^4 p \int d^4 q \frac{1}{p^2 q^2} \frac{1}{q^2 - r} \frac{1}{(p - q)^2 - 1} \frac{1}{p^2 - t}, \quad (5.17)$$

is a standard two-loop integral, which can then be evaluated using dimensional regularisation, see for instance [47–50]. The closed form for  $I_{2\text{MS}}^{\text{leading}}$  is still fairly lengthy. However, under the approximation that logarithms of the masses of the SM fields and order unity factors can be ignored compared to the logarithms of heavy NP masses, we find the approximate form for  $I_{2\text{MS}}^{\text{leading}}$  given by

$$I_{2\text{MS}}^{\text{leading}} \simeq \frac{\pi^4}{m_{\tilde{R}_2}^2} \left[ -\frac{c_n + \log\left(\frac{m_{\tilde{R}_2}^2}{m_W^2}\right) + \frac{1}{2} \log^2\left(\frac{m_{\tilde{R}_2}^2}{m_W^2}\right)}{m_{\tilde{R}_2}^2} + \frac{c_n + \log\left(\frac{m_{S_1}^2}{m_W^2}\right) + \frac{1}{2} \log^2\left(\frac{m_{S_1}^2}{m_W^2}\right)}{m_{S_1}^2} \right], \quad (5.18)$$

where  $c_n \equiv 1 + \pi^2/3$  and we have taken the limit of vanishing  $m_u$  after evaluating the integrations in Eq. (5.16). The approximation for the neutrino mass above matches very

well with the full model exact loop computation of Eq. (4.7), in the limit of the hierarchical new physics scales being much heavier than the SM masses in the loops. Note that while the above approximation works well when  $m_{\tilde{R}_2} \gg m_{S_1}$ , it leads to a suppression with respect to the full model loop computation when  $m_{\tilde{R}_2} \sim m_{S_1}$ . This is due to the cancellation of the symmetric structure in the square bracket in Eq. (5.18). This apparent mismatch can be mitigated by making Eq. (5.18) symmetric by replacing  $m_{\tilde{R}_2}^2$  by  $(m_{\tilde{R}_2}^2 - m_{S_1}^2)$  in the prefactor, which is the form that we will use hereafter.

### 5.3 Generalised simplified multi-scale results for radiative neutrino masses

Given the above discussion, showing the effectiveness of the dimensional regularisation based approach, we can now generalise our results for any tree-level realisation of the dimension-7 SMEFT operators leading to loop-level neutrino masses via diagrams shown in Fig. 6. Depending on the actual realisation there can be additional color factors, symmetry factors, and even swapping (between mass and momentum exchange) of some mass scales depending on the projection operators in the diagram. To keep the results as general as possible, we will denote the heavy new bosons in the left diagram of Fig. 6 by  $\Phi_1$  and  $\Phi_2$ . For topology I, the relevant simplified interactions are then given by the Lagrangian

$$\mathcal{L}^I = \mathcal{L}_{\text{SM}} + \mathcal{L}_{\Phi_1}^{\text{kin}} + \mathcal{L}_{\Phi_2}^{\text{kin}} - \lambda_{\Phi_1} f L \Phi_1^* - \lambda_{\Phi_2} f L \Phi_2^* - \mu \Phi_1^* \Phi_2^* H, \quad (5.19)$$

where  $\mu$  is a dimensionful coupling, and  $\mathcal{L}_{\Phi_1}^{\text{kin}}$  and  $\mathcal{L}_{\Phi_2}^{\text{kin}}$  are the kinetic Lagrangians for  $\Phi_1$  and  $\Phi_2$ , respectively. Similarly, for topology II we consider a simplified model that contains one heavy new fermion  $\Psi$  and one heavy new scalar  $\Phi$  interacting with the SM Higgs- and lepton doublets, respectively. This scenario can be described by the simplified Lagrangian

$$\mathcal{L}^{\text{II}} = \mathcal{L}_{\text{SM}} + \mathcal{L}_{\Psi}^{\text{kin}} + \mathcal{L}_{\Phi}^{\text{kin}} - \lambda_f f L \Phi^* - y_{\Psi} f \bar{\Psi} H, \quad (5.20)$$

where  $\lambda_f$  and  $y_{\Psi}$  are dimensionless coupling constants, and where  $f$  is a SM fermion.

The two new heavy BSM fields that are introduced in either case will be assumed to have a large hierarchy. By neglecting the masses for the SM fermion in the loop and any color or symmetry factors, we can approximate the radiative neutrino mass generated in topology I by

$$(m_{\nu})_{ij}^{\text{I}} \approx \frac{1}{16\pi^2} \frac{v\mu}{m_{\Phi_1}^2 - m_{\Phi_2}^2} \log \left( \frac{m_{\Phi_1}^2}{m_{\Phi_2}^2} \right) (\lambda_{\Phi_1} M_f \lambda_{\Phi_2}^T + \lambda_{\Phi_2} M_f^T \lambda_{\Phi_1}^T)_{ij}, \quad (5.21)$$

and topology II by

$$(m_{\nu})_{ij}^{\text{II}} \approx \frac{1}{16\pi^2} \frac{v}{m_{\Psi}^2 - m_{\Phi}^2} \log \left( \frac{m_{\Psi}^2}{m_{\Phi}^2} \right) (\lambda_f M_f y_{\Psi} M_{\Psi}^T \lambda_{\Psi}^T + \lambda_{\Psi} M_{\Psi} y_{\Psi}^T M_f^T \lambda_f^T)_{ij}. \quad (5.22)$$

Here  $m_{\alpha}$  for  $\alpha \in \{\Phi, \Psi, \Phi_1, \Phi_2\}$  is the mass of the corresponding heavy BSM field, and  $M_f$  and  $M_{\Psi}$  are the diagonal  $3 \times 3$  mass matrices for the SM fermion  $f$  and BSM fermion  $\Psi$

respectively, where we have assumed that  $\Psi$  has three generations. At two-loop we have

$$(m_\nu)_{ij}^{\text{I, two-loop}} \approx \frac{1}{(16\pi^2)^2} \frac{v^3 \mu}{m_{\Phi_1}^2 - m_{\Phi_2}^2} [f_\ell(m_{\Phi_1}, m_W) - f_\ell(m_{\Phi_2}, m_W)] \times (\lambda_{\Phi_1} M_f \lambda_{\Phi_2}^T + \lambda_{\Phi_2} M_f^T \lambda_{\Phi_1}^T)_{ij} \quad (5.23)$$

in topology I and

$$(m_\nu)_{ij}^{\text{II, two-loop}} \approx \frac{1}{(16\pi^2)^2} \frac{v^3}{m_\Psi^2 - m_\Phi^2} [f_\ell(m_\Psi, m_W) - f_\ell(m_\Phi, m_W)] \times (\lambda_f M_f y_\Psi M_\Psi^T \lambda_\Psi^T + \lambda_\Psi M_\Psi y_\Psi^T M_f^T \lambda_f^T)_{ij} \quad (5.24)$$

in topology II, where the function  $f_\ell(m_\chi, m_W)$  is defined as

$$f_\ell(m_\chi, m_W) \equiv \frac{\left(1 + \frac{\pi^2}{3}\right) + \log\left(\frac{m_\chi^2}{m_W^2}\right) + \frac{1}{2} \log^2\left(\frac{m_\chi^2}{m_W^2}\right)}{m_\chi^2}. \quad (5.25)$$

Besides generating radiative neutrino masses, the simplified models discussed here will also lead to other phenomenological processes involving the  $\Delta L = 2$  dimension-7 operators (cf. Ref. [8]). The corresponding Wilson coefficients can be written as

$$C_{ij}^{\text{I}} = \frac{\mu (\lambda_{\Phi_1} \lambda_{\Phi_2})_{ij}}{m_{\Phi_1}^2 m_{\Phi_2}^2} \quad (5.26)$$

for topology I, and

$$C_{ij}^{\text{II}} = \frac{(\lambda_\Psi y_\Psi \lambda_f)_{ij}}{m_\Phi^2 m_\Psi} \quad (5.27)$$

for topology II. The relevant phenomenology is briefly discussed in Sec. 6.

The results for the new simplified multi-scale approach as derived in the previous subsection and generalised in this section, applied to the model example discussed in Sec. 4.2, are shown in Fig. 4 using red solid lines. Compared to the cut-off regularisation based estimates shown in green solid lines, it is easy to see that our simplified multi-scale prescription provides a much closer estimate of the exact model results. For one-loop radiative neutrino masses the improvement is clearly visible when the ratio between the NP scales exceeds a few. On the other hand, for the two-loop radiative neutrino mass diagram, the results are even more striking. The disagreement obtained between the cut-off regularisation based estimate and the model stems not only from the hierarchy between the new physics scales, but also from an unphysical cancellation of the new physics scales due to cut-off regularisation combined with a relatively poor approximation in the presence of an additional loop of electroweak gauge bosons. The treatment of this type of radiative neutrino masses using the simplified multi-scale approach leads to a very accurate approximation of the exact results in spite of a number of approximations and simplifications with respect to the exact full model computation, thereby demonstrating the simplicity and power of the simplified multi-scale approach. In what follows, we now show that allowing for the masses of the

heavy new physics fields realising higher dimensional LNV operators to be independent parameters opens up new parts of phenomenological parameter space which can be explored and confronted with a number of LNV experimental observables.

## 6 Phenomenology of UV-completions at dimension-7

In this section we discuss the different constraints on the simplified models that appear as UV-completions of the  $\Delta L = 2$  dimension-7 operators, including collider constraints as well as low-energy observables such as neutrinoless double beta ( $0\nu\beta\beta$ ) decay, and compare these constraints to radiative neutrino mass generation using the different approaches discussed above. In Figs. 7 and 8 we show the constraints in the parameter space spanned by the two heavy scales, for tree-level UV-completions of the four-fermion  $\Delta L = 2$  dimension-7 effective operators for both topologies I and II. We chose this plane since it best highlights the effects of a varying hierarchy in the internal degrees of freedom. Here all dimensionless couplings are set to unity, and the dimensionful coupling  $\mu$  is parametrized as  $\mu = \max(m_{\Phi_1}, m_{\Phi_2})$ . We focus on operators  $\mathcal{O}_{\bar{Q}uLLH}$ ,  $\mathcal{O}_{\bar{d}LueH}$ ,  $\mathcal{O}_{\bar{d}LQLH1}$ ,  $\mathcal{O}_{\bar{d}LQLH2}$ , and  $\mathcal{O}_{\bar{e}LLLH}$  in this section.

In Ref. [8], we presented the collider limits for dimension-7 operators when the relevant interactions are taken as point-like, i.e. when the heavy NP degrees of freedom are not produced on-shell as resonances. The purple regions in Figs. 7 and 8, corresponding to constraints from searches for  $pp \rightarrow \ell^+\ell^+jj$  at the LHC, are cut off at the lower ends in both NP mass-variables due to the constraint  $M < 900$  GeV as required in order to ensure the validity of the EFT-approach (c.f. Ref. [8]). The resulting constrained areas are comparatively small, and always fully excluded by the flavour-universal neutrino mass constraint. For operators  $\mathcal{O}_{\bar{d}LQLH1}$  and  $\mathcal{O}_{\bar{d}LQLH2}$  the area vanishes completely, as seen in Figs. 7 (center row) and Fig. 8 (top row), respectively, since the constraint is lower than the EFT validity scale for all NP masses. However, the cross section for  $pp \rightarrow \ell^+\ell^+jj$  may be enhanced by on-shell mediators, such as e.g. in the Keung-Senjanović process [51].

Under the assumption that the  $\Delta L = 2$  dimension-7 operators are generated at tree-level, collider constraints on the individual heavy fields that generate a given operator will translate into constraints on the Wilson coefficient of the operator itself. Collider searches for new heavy fields are typically most sensitive when the field can be created on-shell as a resonance. However, such resonant searches are typically dependent on model parameters. Instead, constraints on the underlying new heavy particles in the different UV-completions can also be derived from global fits of dimension-6 operators [52, 53]. The constraints obtained from this method are typically within an order of magnitude of the constraints from resonant searches. We use the 95% C.L. constraints on the masses of the different new fields that appear in the UV-completions of  $\Delta L = 2$  dimension-7 operators from Refs. [52–54]. For these constraints we assume flavour universality and take the most stringent constraints for the cases where several results are available in the literature. In the following analysis, in order to reduce the number of parameters, we set all couplings to unity. The green regions in Figs. 7 and 8 are excluded by global fits of dimension-6 operators for LHC searches, translated into limits on the corresponding tree-level UV-completions [52, 53]. The lightest



Cuts for $pp \rightarrow \mu^\pm \mu^\pm jj$ at $\sqrt{s} = 13$ TeV	
Object selection cuts	
$p_T^{\mu^{1(2)}} > 25$ GeV	$p_T^{j^{1(2)}} > 20$ GeV
$ \eta^{\mu^{1(2)}}  < 2.5$	$ \eta^{j^{1(2)}}  < 2.5$
Track-to-vertex association cuts	
$ z_0 \sin \theta  < 5$ mm	$ d_0  < 1$ $\mu\text{m}$
Signal region cuts	
$p_T^{\mu^{\text{leading}}} > 40$ GeV	$p_T^{j^{1(2)}} > 100$ GeV
$H_T > 400$ GeV	$\Delta R_{\mu\mu} < 3.9$ GeV
$m_{\mu^1 \mu^2} > 400$ GeV	$m_{j^1 j^2} > 110$ GeV

**Table 6:** Cuts used to calculate the number of  $pp \rightarrow \ell^\pm \ell^\pm$  events at ATLAS in the  $\tilde{R}_2$ - $S_1$  leptoquark model, following Ref. [55].

green area is excluded by the most stringent constraint, and the darker green area by the least stringent.

The model example discussed in Sec. 4.2 is subject to constraints from leptoquark searches at the LHC. The leptoquarks  $S_1$  and  $\tilde{R}_2$  both lead to distinct signatures at the LHC, where they can be produced e.g. via pair production  $pp \rightarrow \text{LQ LQ}$  or single production  $pp \rightarrow \ell \text{LQ}$ , see e.g. Refs. [56, 57]. Using these modes, the masses of  $\tilde{R}_2$  and  $S_1$  have been constrained to  $m_{\tilde{R}_2} < 3.4$  TeV and  $m_{S_1} < 4.6$  TeV, respectively, at 95% C.L. [58]. However, the above-mentioned processes are not LNV by two units  $\Delta L = 2$ , and therefore they do not directly correspond to Majorana neutrino masses. In order to probe the latter scenario, an overall  $\Delta L = 2$  process such as  $pp \rightarrow \ell^\pm \ell^\pm jj$  would need to be searched for. Such an analysis was performed for the dimension-7 LNV operators in Ref. [8] from a model-independent perspective, leading to constraints  $\Lambda_{\text{LNV}} > 1.1$  TeV on both of the operators that are generated in the  $\tilde{R}_2$ - $S_1$  model, where  $\Lambda_{\text{LNV}}$  is the corresponding NP scale. However, these operator-based constraints could be an underestimate of what the actual model-dependent constraints would be, since a given model can lead to resonant enhancements. To find the model-dependent constraints on the  $\tilde{R}_2$ - $S_1$  model coming from  $pp \rightarrow \ell^\pm \ell^\pm jj$  searches at the LHC, we implement the model using FEYNRULES [59] and calculate the cross section with MADGRAPH5 [60], including PYTHIA8 [61] for hadronisation and using the PDF set NNPDF30 provided by LHAPDF6 [62], after which we perform detector simulation using DELPHES3 [63] with the cuts shown in Tab. 6, and compare with the ATLAS results [55] for LHC Run 2 at  $\sqrt{s} = 13$  TeV. We perform this analysis for  $\mu = \max(m_{\tilde{R}_2}, m_{S_1})$  in two scenarios: a)  $g_1 = g_2 = 1$  and  $g_3 = 0$ , corresponding to  $\mathcal{O}_{\tilde{d}LQLH1}$ , and b)  $g_1 = g_3 = 1$  and  $g_2 = 0$ , corresponding to  $\mathcal{O}_{\tilde{d}LueH}$ . For a vanishing hierarchy, such that  $m_{\tilde{R}_2} = m_{S_1} \equiv \Lambda_{\text{LNV}}$ ,

and at 95% C.L., we find  $\Lambda_{\text{LNV}} > 3.1$  TeV in both scenarios a) and b).

There is a variety of ways that LNV can be probed at low energies, as was discussed in detail in Ref. [8]. The most stringent bounds generally stem from neutrinoless double beta ( $0\nu\beta\beta$ ) decay searches, which, however, can probe only the first-generation couplings. Therefore, in NP models that dominantly couple the second- or third generation fermions,  $0\nu\beta\beta$  decay searches might still not lead to any signals. In such models, it may be rare kaon decays that provide the first hints of LNV [39, 64, 65]. Nonetheless, at leading order and within dimension-7 SMEFT, these processes constrain only operator  $\mathcal{O}_{\bar{d}LQLH1}$ . Further, operator  $\mathcal{O}_{\bar{e}LLH}$  does not lead to  $0\nu\beta\beta$  decay (at tree-level) and may instead be probed in lepton-number-violating rare muon decays [66]. Other observables are not discussed in this work due to them being generally sub-dominant, e.g. coherent elastic neutrino-nucleus scattering (CE $\nu$ NS), long-baseline neutrino oscillation,  $\mu^-$  to  $e^+$  conversion, and other LNV meson decays such as  $K^+ \rightarrow \pi^- \ell^+ \ell^+$  or  $B \rightarrow K \nu \nu$  (see Ref. [8]). The orange areas are excluded by  $0\nu\beta\beta$  decay, and blue shows the exclusion from rare kaon decays for  $\mathcal{O}_{\bar{d}LQLH1}$  (Fig. 7 center row), and magenta shows the exclusion from rare muon decays for  $\mathcal{O}_{\bar{e}LLH}$  (Fig. 7 bottom row).

The red regions in Figs. 7 and 8 show the area of parameter space where the sum of neutrino masses is larger than the limit obtained from the KATRIN experiment [67]<sup>3</sup> following the simplified multi-scale approach described in Sec. 5. Note that the constraint from KATRIN is set on  $m_\nu^{\text{KATRIN}}$  where  $(m_\nu^{\text{KATRIN}})^2 = \sum_i |U_{ei}|^2 m_i^2 < (0.45 \text{ eV})^2$  [69], where  $U$  is the PMNS matrix. We translate this into a limit on the sum of neutrino masses  $\text{Tr } \hat{m}_\nu$  by using the central values of the neutrino mixing angles as well as the mass splittings  $\Delta m_{12}^2 = 7.49 \times 10^{-5} \text{ eV}^2$  and  $\Delta m_{31}^2 = 2.513 \times 10^{-3} \text{ eV}^2$  given by NUFIT v6.0 [42], assuming normal ordering, and solving for the free parameter  $m_1$  (the lightest neutrino mass), such that

$$|U_{e1}|^2 m_1^2 + |U_{e2}|^2 (m_1^2 + \Delta m_{12}^2) + |U_{e3}|^2 (m_1^2 + \Delta m_{13}^2) < (m_\nu^{\text{KATRIN}})^2. \quad (6.1)$$

A lower limit can be obtained by setting the lowest neutrino mass  $m_1$  to zero. The area between these two limits is shown as a striped red region in Figs. 7 and 8. The black striped region shows the corresponding neutrino mass constraints using the conventional cut-off approximation. Note that the dip in the top-left part of the neutrino mass constraint for topology I comes from our choice of  $\mu = \max(m_{\Phi_1}, m_{\Phi_2})$ .

In Figs. 7 and 8 we see that the constraint on 1-loop neutrino masses using the cut-off estimate (black striped area) generally only agrees with our simplified model approach (red striped area) for a vanishing hierarchy, i.e. at the point where the two masses are approximately equal (along the diagonal from bottom left to top right). For a larger hierarchy the disagreement increases, which is also what was found in the comparison in Fig. 4. Fig. 8 corresponds to operators for which the neutrino mass is generated at 2-loop order. Here we see that the cut-off estimate does not reproduce the results of our more accurate simplified-model approach for most of the parameter space, as also seen in Fig. 4. One reason for this mismatch is that the 2-loop mass generally depends on all mass scales involved, rather than

<sup>3</sup>Note that we do not use the corresponding PLANCK limits [68] due to their dependence on the underlying cosmological model.

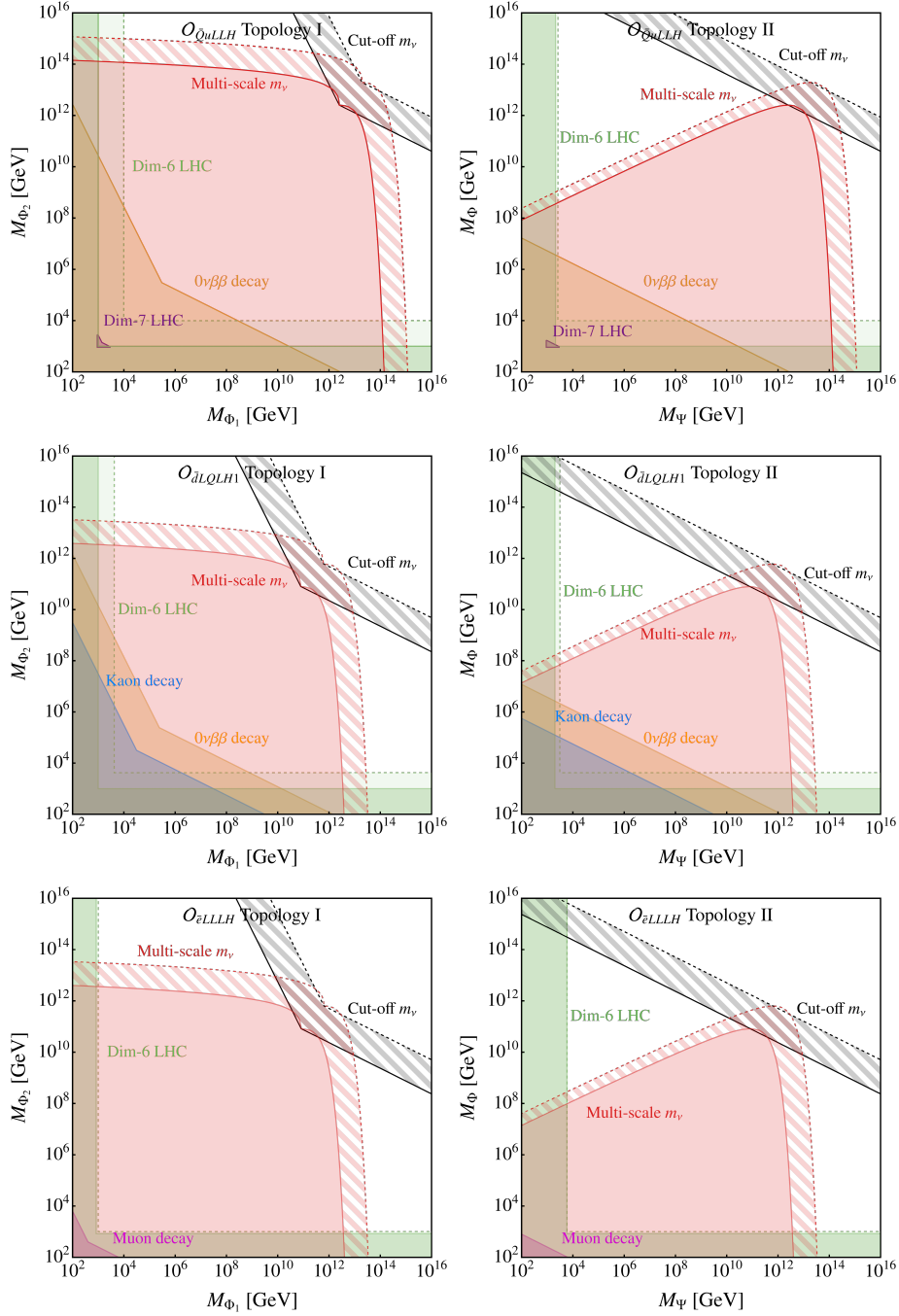


**Figure 7:** Parameter space for operator  $\mathcal{O}_{\bar{Q}uLLH}$  (top row),  $\mathcal{O}_{\bar{d}LQLH1}$  (center row), and  $\mathcal{O}_{\bar{e}LLLH}$  (bottom row) in topology I (left column) and topology II (right column). The red and black areas correspond to two-scale and cut-off neutrino masses, where the striped area leads to the observed neutrino mass and the solid area is excluded. We consider normal ordering of neutrino masses. The orange, blue and magenta areas correspond to  $0\nu\beta\beta$  decay, rare kaon decay and rare muon decay, while green and purple correspond to dim-6 and LNV dim-7 operators at the LHC, respectively.

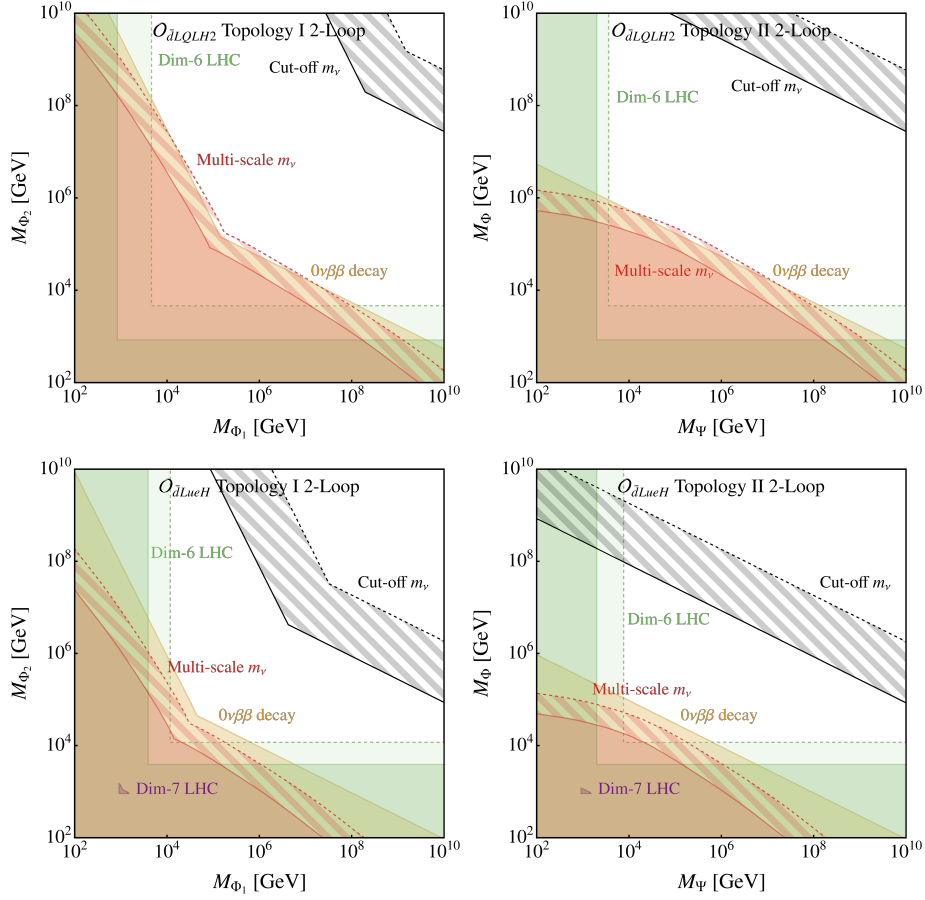


**Figure 8:** Same as Fig. 7, but for operator  $\mathcal{O}_{\bar{d}LQLH_2}$  (top row) and  $\mathcal{O}_{\bar{d}LueH}$  (bottom row).

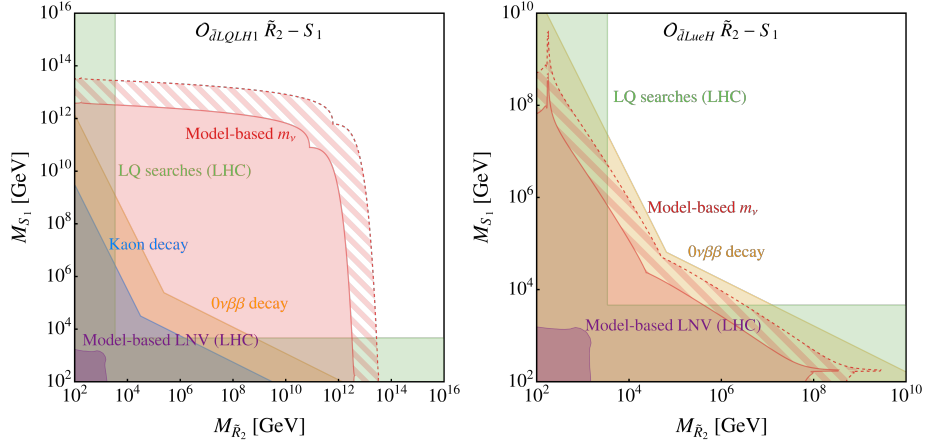


**Figure 9:** Same as Fig. 7, but for the  $\tilde{R}_2 - S_1$  model described in Sec. 4.2.

just the highest scale as was our approximation in the 1-loop case. We further see that the regions which lead to the observed neutrino mass are generally excluded by  $0\nu\beta\beta$  decay.

For some operators, the single-particle limits from global fits of LHC results (green

regions) roughly overlap with the  $0\nu\beta\beta$  and neutrino mass constraints simultaneously, in regions of parameter space where one field is significantly more massive than the other, i.e. where there is a large hierarchy.

In Fig. 9 we show the different constraints in the leptoquark model presented in Sec. 4.2, for the realisation of operators  $\mathcal{O}_{\bar{d}LQLH1}$  (left) and  $\mathcal{O}_{\bar{d}LueH}$  (right). Note that for the latter case, the neutrino mass is generated at 2-loop order, while at 1-loop as in the former. The different colored areas correspond to experimental constraints similar to Figs. 7 and 8, i.e. green, purple, orange, blue and red correspond to direct searches for  $\tilde{R}_2$  and  $S_1$ , LNV at the LHC,  $0\nu\beta\beta$  decay, rare kaon decay, and neutrino masses, respectively, while the striped red areas correspond to the observed neutrino masses. The two different operators are generated by two different couplings of  $S_1$  to the SM. In both cases, the limits coming from LNV searches at the LHC (purple) are subdominant compared to direct searches (green) for the whole parameter space. For comparisons with our simplified model approach, the corresponding figures are Fig. 7 (center left) for Fig. 9 (left) and Fig. 8 (bottom left) for Fig. 9 (right).

The accuracy of the simplified multi-scale approach introduced in Sec. 5 can be, again, verified by its comparison with the UV-complete scenario. Specifically, the neutrino-mass constraints shown in red in the left-center panel of Fig. 7 and in the left-bottom panel of Fig. 8 are in excellent agreement with the bounds obtained from the full model depicted in Fig. 9, left and right panel, respectively. We also see in Figs. 7 and 8 that a hierarchy in the internal degrees of freedom of a given UV-completion of a dimension-7  $\Delta L = 2$  operator has a significant effect on the size of the available parameter space. Unlike the naive single-scale cut-off-regularisation-based limits, the more realistic neutrino mass bounds obtained by the simplified multi-scale approach open up viable regions of parameter space within potential reach of LHC searches and/or future  $0\nu\beta\beta$  decay experiments.

## 7 Conclusions

In this work we have extended the phenomenological investigations of dimension-7  $\Delta L = 2$  operators in the framework of SMEFT by analyzing their UV-completions, in particular, in relation to the generation of the observed neutrino masses. Generally, dimension-7 lepton-number-violating interactions are, following the usual EFT paradigm, expected to be more suppressed than the well-known dimension-5 Weinberg operator. However, in UV scenarios without the seesaw fields these operators can provide the leading contribution to LNV processes and provide a valuable insight into radiative Majorana neutrino mass models.

After obtaining the full list of tree-level UV-completions of dimension-7  $\Delta L = 2$  operators, we identified the radiative neutrino Majorana mass topologies corresponding to these UV-completions, and provided approximate expressions for the value of the neutrino mass in both scenarios. When doing so we have used a dimensional-regularisation-based approach to study neutrino mass contributions in a multiscale setup, ensuring a more robust analysis and allowing for realistic description in presence of a hierarchy among new fields. We then compared our results to a leptoquark model example, for which we find very good agreement and a significant improvement over conventional approximations of the neutrino

mass corresponding to dimension-7 operators employing naive cut-off-based regularisation. Most notably, we showed that a hierarchy in the internal degrees of freedom of an operator will significantly affect the neutrino mass.

As part of the subsequent phenomenological analysis we compared our results to other observables probing LNV, including  $0\nu\beta\beta$  decay and the LHC. Among other things we found that there are regions of parameter space for most operators that successfully generate the observed neutrino mass while being close to the experimental reach of both the LHC and  $0\nu\beta\beta$  decay. These regions generally involve a large internal hierarchy, and as such have evaded the attention in previous studies assuming a common scale of NP. In this way, our findings provide valuable guidance for future experimental efforts aimed at probing LNV and searching for BSM physics.

## Acknowledgements

K. F. acknowledges support from the Japan Society for the Promotion of Science (JSPS) Grant-in-Aid for Scientific Research B (No. 21H01086). L. G. acknowledges support from the Dutch Research Council (NWO), under project number VI.Veni.222.318; from Charles University through project PRIMUS/24/SCI/013; from the National Science Foundation, Grant PHY-1630782, and the Heising-Simons Foundation, Grant 2017-228. L. G. is also thankful to Instituto de Física Corpuscular (IFIC) for the hospitality provided during his visit that led to finalization of this project. J. H. acknowledges support by the Cluster of Excellence “Precision Physics, Fundamental Interactions, and Structure of Matter” (PRISMA<sup>+</sup> EXC 2118/1) funded by the Deutsche Forschungsgemeinschaft (DFG, German Research Foundation) within the German Excellence Strategy (Project No. 390831469). C. H. is funded by the Generalitat Valenciana under Plan Gen-T via CDEIGENT grant No. CIDEIG/2022/16. C. H. also acknowledges support from the Spanish grants PID2023-147306NB-I00 and CEX2023-001292-S (MCIU/AEI/10.13039/501100011033), as well as CIPROM/2021/054 (Generalitat Valenciana). K. F., J. H. and C. H. also acknowledge support from the Emmy Noether grant "Baryogenesis, Dark Matter and Neutrinos: Comprehensive analyses and accurate methods in particle cosmology" (HA 8555/1-1, Project No. 400234416) funded by the Deutsche Forschungsgemeinschaft (DFG, German Research Foundation).

## A Covariant derivative expansion

In order to relate the  $\Delta L = 2$  operators to the underlying tree-level UV-completions we here employ the covariant derivative expansion formalism (CDE) [28] following Ref. [18]. In this Appendix we show the calculations corresponding to the results presented in Sec. 2, for a scalar, fermion, and vector field, respectively.

## A.1 Scalar field

A general Lagrangian that contain both light fields  $\pi_i$  and heavy complex scalar fields  $\Phi$  can be written as

$$\mathcal{L}_S \supset \mathcal{L}_\Phi^{\text{int}} + \mathcal{L}_\Phi^{\text{kin}} = \left( \Phi \frac{\partial \mathcal{L}_\Phi^{\text{int}}}{\partial \Phi} + \text{h.c.} \right) + \Phi^* (-D^2 - m_\Phi^2) \Phi + \mathcal{O}(\Phi^3). \quad (\text{A.1})$$

Here  $D$  is a covariant derivative, and we have neglected terms quadratic in  $\Phi$ . Evaluating the linearised equations of motion (EOM) for  $\Phi$  then leads to

$$(-D^2 - m_\Phi^2) \Phi = -\frac{\partial \mathcal{L}_\Phi^{\text{int}}}{\partial \Phi^*} + \mathcal{O}(\Phi^2), \quad (\text{A.2})$$

which we can solve using the classical field

$$\Phi_{\text{cl}} = \frac{1}{D^2 + m_\Phi^2} \frac{\partial \mathcal{L}_\Phi^{\text{int}}}{\partial \Phi^*}. \quad (\text{A.3})$$

Expanding in  $D^2/m_\Phi^2$  we have

$$\Phi_{\text{cl}} = \frac{1}{m_\Phi^2} \left( 1 + \frac{D^2}{m_\Phi^2} \right)^{-1} \frac{\partial \mathcal{L}_\Phi^{\text{int}}}{\partial \Phi^*} = \left( \frac{1}{m_\Phi^2} - \frac{D^2}{m_\Phi^4} + \dots \right) \frac{\partial \mathcal{L}_\Phi^{\text{int}}}{\partial \Phi^*}. \quad (\text{A.4})$$

Substituting the classical field into Eq. (A.1) gives us a series of interaction terms

$$\mathcal{L}_{\text{eff}} \supset \mathcal{L}_{\text{eff}}^\Phi = \frac{\partial \mathcal{L}_\Phi^{\text{int}}}{\partial \Phi} \left( \frac{1}{m_\Phi^2} - \frac{D^2}{m_\Phi^4} + \dots \right) \frac{\partial \mathcal{L}_\Phi^{\text{int}}}{\partial \Phi^*}. \quad (\text{A.5})$$

This expression contains an effective Lagrangian that is independent of the heavy scalar field  $\Phi$ , but that does depend on the interactions of  $\Phi$  with other fields, both light and heavy, corresponding to the derivatives  $\partial \mathcal{L}_\Phi^{\text{int}} / \partial \Phi^{(*)}$ .

## A.2 Fermion field

For a heavy Dirac fermion field  $\Psi \equiv (\chi_\alpha, \eta^{\dagger\dot{\alpha}})^T$  we have

$$\begin{aligned} \mathcal{L}_S &\supset i\bar{\Psi} \not{D} \Psi - m_\Psi \bar{\Psi} \Psi + \left( \Psi \frac{\partial \mathcal{L}_\Psi^{\text{int}}}{\partial \Psi} + \text{h.c.} \right) \\ &= i\chi_\alpha^\dagger D^{\dot{\alpha}\beta} \chi_\beta + i\eta^\alpha D_{\alpha\dot{\beta}} \eta^{\dagger\dot{\beta}} + \left( \chi_\alpha \frac{\partial \mathcal{L}_\Psi^{\text{int}}}{\partial \chi_\alpha} + \eta^\alpha \frac{\partial \mathcal{L}_\Psi^{\text{int}}}{\partial \eta^\alpha} - m_\Psi \eta^\alpha \chi_\alpha + \text{h.c.} \right). \end{aligned} \quad (\text{A.6})$$

Here we have used

$$D^{\dot{\alpha}\beta} \equiv D^\mu \bar{\sigma}_\mu^{\dot{\alpha}\beta}, \quad D_{\alpha\dot{\beta}} \equiv D^\mu \sigma_{\mu\alpha\dot{\beta}}. \quad (\text{A.7})$$

The second term in Eq. (A.6) can be written in the form of the first using integration by parts,

$$i\eta^\alpha D_{\alpha\dot{\beta}} \eta^{\dagger\dot{\beta}} = -i(D^\mu \eta^\alpha) \sigma_{\mu\alpha\dot{\beta}} \eta^{\dagger\dot{\beta}}. \quad (\text{A.8})$$

After applying a Fierz transformation

$$-i(D^\mu \eta^\alpha) \sigma_{\mu\alpha\dot{\beta}} \eta^{\dagger\dot{\beta}} = i\eta_{\dot{\beta}}^\dagger \bar{\sigma}_\mu^{\dot{\beta}\alpha} D^\mu \eta_\alpha = i\eta_{\dot{\beta}}^\dagger D^{\dot{\beta}\alpha} \eta_\alpha, \quad (\text{A.9})$$

we can write the EOM as

$$iD^{\dot{\alpha}\beta} \chi_\beta - m_\Psi \eta^{\dagger\dot{\alpha}} + \frac{\partial \mathcal{L}_\Psi^{\text{int}}}{\partial \chi_{\dot{\alpha}}^\dagger} = 0, \quad (\text{A.10})$$

$$iD^{\dot{\alpha}\beta} \eta_\beta - m_\Psi \chi^{\dagger\dot{\alpha}} + \frac{\partial \mathcal{L}_\Psi^{\text{int}}}{\partial \eta_{\dot{\alpha}}^\dagger} = 0, \quad (\text{A.11})$$

where in Eq. (A.10) we can be solve for  $\eta_{\dot{\beta}}^\dagger$ ,

$$\eta_{\dot{\beta}}^\dagger = \frac{1}{m_\Psi} \epsilon_{\dot{\beta}\dot{\alpha}} \left( iD^{\dot{\alpha}\beta} \chi_\beta + \frac{\partial \mathcal{L}_\Psi^{\text{int}}}{\partial \chi_{\dot{\alpha}}^\dagger} \right) = i \frac{1}{m_\Psi} \epsilon_{\dot{\beta}\dot{\alpha}} D^{\dot{\alpha}\beta} \chi_\beta + \frac{1}{m_\Psi} \frac{\partial \mathcal{L}_\Psi^{\text{int}}}{\partial \chi^{\dagger\dot{\beta}}}. \quad (\text{A.12})$$

Taking the complex conjugate of Eq. (A.11) now leads to

$$\frac{1}{m_\Psi} D^{\dot{\beta}\alpha} \epsilon_{\dot{\beta}\dot{\alpha}} D^{\dot{\alpha}\beta} \chi_\beta + i \frac{1}{m_\Psi} D^{\dot{\beta}\alpha} \frac{\partial \mathcal{L}_\Psi^{\text{int}}}{\partial \chi^{\dagger\dot{\beta}}} - m_\Psi \chi^\alpha + \frac{\partial \mathcal{L}_\Psi^{\text{int}}}{\partial \eta_\alpha} = 0. \quad (\text{A.13})$$

Expressing the first term in Eq. (A.13) using the field strength

$$X_\alpha{}^\beta \equiv X^{\mu\nu} \sigma_{\nu\alpha\dot{\gamma}} \bar{\sigma}_\mu^{\dot{\gamma}\beta} = -i [D^\mu, D^\nu] \sigma_{\nu\alpha\dot{\gamma}} \bar{\sigma}_\mu^{\dot{\gamma}\beta} \quad (\text{A.14})$$

and the relation

$$\begin{aligned} D^{\dot{\beta}\alpha} \epsilon_{\dot{\beta}\dot{\alpha}} D^{\dot{\alpha}\beta} &= D^\mu D^\nu \bar{\sigma}_\mu^{\dot{\alpha}\beta} \epsilon_{\dot{\beta}\dot{\alpha}} \bar{\sigma}_\nu^{\dot{\beta}\alpha} \\ &= D^\mu D^\nu \epsilon^{\beta\gamma} \sigma_{\mu\gamma\dot{\beta}} \bar{\sigma}_\nu^{\dot{\beta}\alpha} \\ &= D^\mu D^\nu \epsilon^{\beta\gamma} (\eta_{\mu\nu} \delta_\gamma^\alpha - 2i(\sigma_{\mu\nu})_\gamma^\alpha) \\ &= D^2 \epsilon^{\beta\alpha} + \frac{i}{2} \epsilon^{\beta\gamma} X_\gamma{}^\alpha, \end{aligned} \quad (\text{A.15})$$

where

$$(\sigma_{\mu\nu})_\alpha{}^\beta \equiv \frac{i}{4} \left( \sigma_{\mu\alpha\dot{\gamma}} \bar{\sigma}_\nu^{\dot{\gamma}\beta} - \sigma_{\nu\alpha\dot{\gamma}} \bar{\sigma}_\mu^{\dot{\gamma}\beta} \right), \quad (\bar{\sigma}_{\mu\nu})^{\dot{\alpha}\dot{\beta}} \equiv \frac{i}{4} \left( \bar{\sigma}_\mu^{\dot{\alpha}\gamma} \sigma_{\nu\gamma\dot{\beta}} - \bar{\sigma}_\nu^{\dot{\alpha}\gamma} \sigma_{\mu\gamma\dot{\beta}} \right). \quad (\text{A.16})$$

then leads to

$$m_\Psi^2 \left( \frac{-D^2 \epsilon^{\alpha\delta} - \frac{i}{2} X_\gamma{}^\alpha \epsilon^{\gamma\delta}}{m_\Psi^2} - \epsilon^{\alpha\delta} \right) \chi_\delta + iD^{\dot{\beta}\alpha} \frac{\partial \mathcal{L}_\Psi^{\text{int}}}{\partial \chi^{\dagger\dot{\beta}}} + m_\Psi \frac{\partial \mathcal{L}_\Psi^{\text{int}}}{\partial \eta_\alpha} = 0 \quad (\text{A.17})$$



which we can solve using the classical fermion field

$$\begin{aligned}
(\chi_{\text{cl}})_\delta &= \frac{1}{m_\Psi^2} \left( \frac{-D^2 \epsilon^{\alpha\delta} - \frac{i}{2} X_\gamma^\alpha \epsilon^{\gamma\delta}}{m_\Psi^2} - \epsilon^{\alpha\delta} \right)^{-1} \left( iD^{\beta\alpha} \frac{\partial \mathcal{L}_\Psi^{\text{int}}}{\partial \chi^{\dagger\beta}} + m_\Psi \frac{\partial \mathcal{L}_\Psi^{\text{int}}}{\partial \eta_\alpha} \right) \\
&= \left( \frac{\epsilon_{\alpha\delta}}{m_\Psi^2} + \frac{D^2 \epsilon_{\alpha\delta} + \frac{i}{2} X_\alpha^\gamma \epsilon_{\gamma\delta}}{m_\Psi^4} + \dots \right) \left( iD^{\beta\alpha} \frac{\partial \mathcal{L}_\Psi^{\text{int}}}{\partial \chi^{\dagger\beta}} + m_\Psi \frac{\partial \mathcal{L}_\Psi^{\text{int}}}{\partial \eta_\alpha} \right).
\end{aligned} \tag{A.18}$$

The classical field  $(\eta_{\text{cl}})_\delta$  can be obtained in an analogous way. We now substitute the fields in Eq. (A.6) to obtain a series of interaction terms

$$\begin{aligned}
\mathcal{L}_{\text{eff}} \supset \mathcal{L}_{\text{eff}}^\Psi &= \frac{\partial \mathcal{L}_\Psi^{\text{int}}}{\partial \chi_\delta} \left( \frac{\epsilon_{\alpha\delta}}{m_\Psi^2} + \frac{D^2 \epsilon_{\alpha\delta} + \frac{i}{2} X_\alpha^\gamma \epsilon_{\gamma\delta}}{m_\Psi^4} + \dots \right) \left( iD^{\beta\alpha} \frac{\partial \mathcal{L}_\Psi^{\text{int}}}{\partial \chi^{\dagger\beta}} + m_\Psi \frac{\partial \mathcal{L}_\Psi^{\text{int}}}{\partial \eta_\alpha} \right) \\
&+ \frac{\partial \mathcal{L}_\Psi^{\text{int}}}{\partial \eta_\delta} \left( \frac{\epsilon_{\alpha\delta}}{m_\Psi^2} + \frac{D^2 \epsilon_{\alpha\delta} + \frac{i}{2} X_\alpha^\gamma \epsilon_{\gamma\delta}}{m_\Psi^4} + \dots \right) \left( iD^{\beta\alpha} \frac{\partial \mathcal{L}_\Psi^{\text{int}}}{\partial \eta^{\dagger\beta}} + m_\Psi \frac{\partial \mathcal{L}_\Psi^{\text{int}}}{\partial \chi_\alpha} \right) + \text{h.c.} \\
&= \frac{\partial \mathcal{L}_\Psi^{\text{int}}}{\partial \Psi} \left( \frac{1}{m_\Psi^2} + \frac{D^2 + \frac{1}{2} X_{\mu\nu} \sigma^{\mu\nu}}{m_\Psi^4} + \dots \right) (i\not{D} + m_\Psi) \frac{\partial \mathcal{L}_\Psi^{\text{int}}}{\partial \Psi},
\end{aligned} \tag{A.19}$$

where we have used

$$\sigma^{\mu\nu} \equiv \frac{i}{2} [\gamma^\mu, \gamma^\nu]. \tag{A.20}$$

For Majorana fields we can use the replacements  $\eta^\alpha \rightarrow \chi^\alpha$  and  $m_\Psi \rightarrow \frac{1}{2} m_\Psi$ .

### A.3 Vector field

A heavy vector field  $\mathbf{V}^\mu$  leads to

$$\mathcal{L}_S \supset -\frac{1}{4} (D_\mu \mathbf{V}_\nu^* - D_\nu \mathbf{V}_\mu^*) (D^\mu \mathbf{V}^\nu - D^\nu \mathbf{V}^\mu) + \frac{1}{2} m_{\mathbf{V}}^2 \mathbf{V}_\mu^* \mathbf{V}^\mu - \frac{\partial \mathcal{L}_{\mathbf{V}}^{\text{int}}}{\partial \mathbf{V}_\mu^*} \mathbf{V}_\mu^*, \tag{A.21}$$

where we have used the field strength  $X^{\mu\nu} = -i [D^\mu, D^\nu]$ . The EOM can be obtained as

$$D^2 \mathbf{V}^\mu - D^\nu D_\nu \mathbf{V}^\mu + m_{\mathbf{V}}^2 \mathbf{V}^\mu - \frac{\partial \mathcal{L}_{\mathbf{V}}^{\text{int}}}{\partial \mathbf{V}_\mu^*} = 0, \tag{A.22}$$

which we solve with the classical vector field

$$\begin{aligned}
(\mathbf{V}_{\text{cl}})_\rho &= (D^2 \eta^{\mu\rho} - D^\nu D_\nu \eta^{\mu\rho} + m_{\mathbf{V}}^2 \eta^{\mu\rho})^{-1} \frac{\partial \mathcal{L}_{\mathbf{V}}^{\text{int}}}{\partial \mathbf{V}_\mu^*} \\
&= \frac{1}{m_{\mathbf{V}}^2} \left( \eta_{\mu\rho} + \frac{D^2 \eta_{\mu\rho} - D_\nu D_\nu \eta^{\nu\rho}}{m_{\mathbf{V}}^2} + \dots \right) \frac{\partial \mathcal{L}_{\mathbf{V}}^{\text{int}}}{\partial \mathbf{V}_\mu^*}.
\end{aligned} \tag{A.23}$$

This solution then leads to a series of interaction terms without the heavy vector field

$$\mathcal{L}_{\text{eff}} \supset \mathcal{L}_{\text{eff}}^{\mathbf{V}} = \frac{\partial \mathcal{L}_{\mathbf{V}}^{\text{int}}}{\partial \mathbf{V}_\nu} \left( \frac{\eta_{\mu\nu}}{m_{\mathbf{V}}^2} + \frac{D^2 \eta_{\mu\nu} - D_\nu D_\nu \eta_{\mu\nu}}{m_{\mathbf{V}}^4} + \dots \right) \frac{\partial \mathcal{L}_{\mathbf{V}}^{\text{int}}}{\partial \mathbf{V}_\mu^*} \tag{A.24}$$

## References

- [1] A. Kobach, *Baryon Number, Lepton Number, and Operator Dimension in the Standard Model*, *Phys. Lett. B* **758** (2016) 455–457, [[1604.05726](#)].
- [2] B. Henning, X. Lu, T. Melia and H. Murayama, *2, 84, 30, 993, 560, 15456, 11962, 261485, ...: Higher dimension operators in the SM EFT*, *JHEP* **08** (2017) 016, [[1512.03433](#)].
- [3] L. Lehman and A. Martin, *Low-derivative operators of the Standard Model effective field theory via Hilbert series methods*, *JHEP* **02** (2016) 081, [[1510.00372](#)].
- [4] B. Henning, X. Lu, T. Melia and H. Murayama, *Hilbert series and operator bases with derivatives in effective field theories*, *Commun. Math. Phys.* **347** (2016) 363–388, [[1507.07240](#)].
- [5] L. Lehman and A. Martin, *Hilbert Series for Constructing Lagrangians: expanding the phenomenologist’s toolbox*, *Phys. Rev. D* **91** (2015) 105014, [[1503.07537](#)].
- [6] J. Fuentes-Martin, J. Portoles and P. Ruiz-Femenia, *Integrating out heavy particles with functional methods: a simplified framework*, *JHEP* **09** (2016) 156, [[1607.02142](#)].
- [7] R. M. Fonseca, *Enumerating the operators of an effective field theory*, *Phys. Rev. D* **101** (2020) 035040, [[1907.12584](#)].
- [8] K. Fridell, L. Gráf, J. Harz and C. Hati, *Probing Lepton Number Violation: A Comprehensive Survey of Dimension-7 SMEFT*, [2306.08709](#).
- [9] J. Herrero-García and M. A. Schmidt, *Neutrino mass models: New classification and model-independent upper limits on their scale*, *Eur. Phys. J. C* **79** (2019) 938, [[1903.10552](#)].
- [10] F. Bonnet, D. Hernandez, T. Ota and W. Winter, *Neutrino masses from higher than  $d=5$  effective operators*, *JHEP* **10** (2009) 076, [[0907.3143](#)].
- [11] P. W. Angel, N. L. Rodd and R. R. Volkas, *Origin of neutrino masses at the LHC:  $\Delta L = 2$  effective operators and their ultraviolet completions*, *Phys. Rev. D* **87** (2013) 073007, [[1212.6111](#)].
- [12] Y. Cai, J. D. Clarke, M. A. Schmidt and R. R. Volkas, *Testing Radiative Neutrino Mass Models at the LHC*, *JHEP* **02** (2015) 161, [[1410.0689](#)].
- [13] J. de Blas, J. C. Criado, M. Perez-Victoria and J. Santiago, *Effective description of general extensions of the Standard Model: the complete tree-level dictionary*, *JHEP* **03** (2018) 109, [[1711.10391](#)].
- [14] R. Cepedello, M. Hirsch and J. C. Helo, *Lepton number violating phenomenology of  $d = 7$  neutrino mass models*, *JHEP* **01** (2018) 009, [[1709.03397](#)].
- [15] R. Cepedello, M. Hirsch and J. C. Helo, *Loop neutrino masses from  $d = 7$  operator*, *JHEP* **07** (2017) 079, [[1705.01489](#)].
- [16] G. Anamiati, O. Castillo-Felisola, R. M. Fonseca, J. C. Helo and M. Hirsch, *High-dimensional neutrino masses*, *JHEP* **12** (2018) 066, [[1806.07264](#)].
- [17] A. De Gouvêa, W.-C. Huang, J. König and M. Sen, *Accessible Lepton-Number-Violating Models and Negligible Neutrino Masses*, *Phys. Rev. D* **100** (2019) 075033, [[1907.02541](#)].
- [18] J. Gargalionis and R. R. Volkas, *Exploding operators for Majorana neutrino masses and beyond*, *JHEP* **01** (2021) 074, [[2009.13537](#)].

- [19] P.-T. Chen, G.-J. Ding and C.-Y. Yao, *Decomposition of  $d = 9$  short-range  $0\nu\beta\beta$  decay operators at one-loop level*, *JHEP* **12** (2021) 169, [[2110.15347](#)].
- [20] U. Banerjee, J. Chakraborty, S. Prakash, S. U. Rahaman and M. Spannowsky, *Effective Operator Bases for Beyond Standard Model Scenarios: An EFT compendium for discoveries*, *JHEP* **01** (2021) 028, [[2008.11512](#)].
- [21] M. Chala and A. Titov, *Neutrino masses in the Standard Model effective field theory*, *Phys. Rev. D* **104** (2021) 035002, [[2104.08248](#)].
- [22] S. Das Bakshi, J. Chakraborty, S. Prakash, S. U. Rahaman and M. Spannowsky, *EFT diagrammatica: UV roots of the CP-conserving SMEFT*, *JHEP* **06** (2021) 033, [[2103.11593](#)].
- [23] Y. Cai, J. Herrero-García, M. A. Schmidt, A. Vicente and R. R. Volkas, *From the trees to the forest: a review of radiative neutrino mass models*, *Front. in Phys.* **5** (2017) 63, [[1706.08524](#)].
- [24] K. S. Babu, P. S. B. Dev, S. Jana and A. Thapa, *Non-Standard Interactions in Radiative Neutrino Mass Models*, *JHEP* **03** (2020) 006, [[1907.09498](#)].
- [25] A. de Gouvea and J. Jenkins, *A Survey of Lepton Number Violation Via Effective Operators*, *Phys. Rev. D* **77** (2008) 013008, [[0708.1344](#)].
- [26] L. Lehman, *Extending the Standard Model Effective Field Theory with the Complete Set of Dimension-7 Operators*, *Phys. Rev. D* **90** (2014) 125023, [[1410.4193](#)].
- [27] Y. Liao and X.-D. Ma, *Renormalization Group Evolution of Dimension-seven Baryon- and Lepton-number-violating Operators*, *JHEP* **11** (2016) 043, [[1607.07309](#)].
- [28] B. Henning, X. Lu and H. Murayama, *How to use the Standard Model effective field theory*, *JHEP* **01** (2016) 023, [[1412.1837](#)].
- [29] K. S. Babu and C. N. Leung, *Classification of effective neutrino mass operators*, *Nucl. Phys. B* **619** (2001) 667–689, [[hep-ph/0106054](#)].
- [30] F. F. Deppisch, L. Graf, J. Harz and W.-C. Huang, *Neutrinoless Double Beta Decay and the Baryon Asymmetry of the Universe*, *Phys. Rev. D* **98** (2018) 055029, [[1711.10432](#)].
- [31] D. Aristizabal Sierra, M. Hirsch and S. G. Kovalenko, *Leptoquarks: Neutrino masses and accelerator phenomenology*, *Phys. Rev. D* **77** (2008) 055011, [[0710.5699](#)].
- [32] I. Doršner, S. Fajfer and N. Košnik, *Leptoquark mechanism of neutrino masses within the grand unification framework*, *Eur. Phys. J. C* **77** (2017) 417, [[1701.08322](#)].
- [33] O. Catà and T. Mannel, *Linking lepton number violation with B anomalies*, [1903.01799](#).
- [34] V. De Romeri, V. M. Lozano and G. Sanchez Garcia, *Neutrino window to scalar leptoquarks: From low energy to colliders*, *Phys. Rev. D* **109** (2024) 055014, [[2307.13790](#)].
- [35] S. Fajfer, L. P. S. Leal, O. Sumensari and R. Z. Funchal, *Correlating  $0\nu\beta\beta$  decays and flavor observables in leptoquark models*, [2406.20050](#).
- [36] P. S. B. Dev, S. Goswami, C. Majumdar and D. Pachhar, *Neutrinoless Double Beta Decay from Scalar Leptoquarks: Interplay with Neutrino Mass and Flavor Physics*, [2407.04670](#).
- [37] C.-K. Chua, X.-G. He and W.-Y. P. Hwang, *Neutrino mass induced radiatively by supersymmetric leptoquarks*, *Phys. Lett. B* **479** (2000) 224–229, [[hep-ph/9905340](#)].
- [38] U. Mahanta, *Neutrino masses and mixing angles from leptoquark interactions*, *Phys. Rev. D* **62** (2000) 073009, [[hep-ph/9909518](#)].

- [39] F. F. Deppisch, K. Fridell and J. Harz, *Constraining lepton number violating interactions in rare kaon decays*, *JHEP* **12** (2020) 186, [[2009.04494](#)].
- [40] K. Fridell, *Leptogenesis and neutrino mass with scalar leptoquarks*, [2411.03282](#).
- [41] K. S. Babu and J. Julio, *Two-Loop Neutrino Mass Generation through Leptoquarks*, *Nucl. Phys. B* **841** (2010) 130–156, [[1006.1092](#)].
- [42] I. Esteban, M. C. Gonzalez-Garcia, M. Maltoni, I. Martinez-Soler, J. a. P. Pinheiro and T. Schwetz, *NuFit-6.0: Updated global analysis of three-flavor neutrino oscillations*, [2410.05380](#).
- [43] A. V. Manohar, *Introduction to Effective Field Theories*, [1804.05863](#).
- [44] D. Zhang, *Renormalization group equations for the SMEFT operators up to dimension seven*, *JHEP* **10** (2023) 148, [[2306.03008](#)].
- [45] D. Zhang, *Revisiting renormalization group equations of the SMEFT dimension-seven operators*, *JHEP* **02** (2024) 133, [[2310.11055](#)].
- [46] K. G. Wilson, *The renormalization group and critical phenomena*, *Rev. Mod. Phys.* **55** (1983) 583–600.
- [47] J. van der Bij and M. J. G. Veltman, *Two Loop Large Higgs Mass Correction to the rho Parameter*, *Nucl. Phys. B* **231** (1984) 205–234.
- [48] K. L. McDonald and B. H. J. McKellar, *Evaluating the two loop diagram responsible for neutrino mass in Babu’s model*, [hep-ph/0309270](#).
- [49] P. W. Angel, Y. Cai, N. L. Rodd, M. A. Schmidt and R. R. Volkas, *Testable two-loop radiative neutrino mass model based on an  $LLQd^cQd^c$  effective operator*, *JHEP* **10** (2013) 118, [[1308.0463](#)].
- [50] D. Aristizabal Sierra, A. Degee, L. Dorame and M. Hirsch, *Systematic classification of two-loop realizations of the Weinberg operator*, *JHEP* **03** (2015) 040, [[1411.7038](#)].
- [51] W.-Y. Keung and G. Senjanovic, *Majorana Neutrinos and the Production of the Right-handed Charged Gauge Boson*, *Phys. Rev. Lett.* **50** (1983) 1427.
- [52] J. Ellis, M. Madigan, K. Mimasu, V. Sanz and T. You, *Top, Higgs, Diboson and Electroweak Fit to the Standard Model Effective Field Theory*, *JHEP* **04** (2021) 279, [[2012.02779](#)].
- [53] A. Crivellin, M. Hoferichter, M. Kirk, C. A. Manzari and L. Schnell, *First-generation new physics in simplified models: from low-energy parity violation to the LHC*, *JHEP* **10** (2021) 221, [[2107.13569](#)].
- [54] J. Ellis, C. W. Murphy, V. Sanz and T. You, *Updated Global SMEFT Fit to Higgs, Diboson and Electroweak Data*, *JHEP* **06** (2018) 146, [[1803.03252](#)].
- [55] ATLAS collaboration, G. Aad et al., *Search for heavy Majorana or Dirac neutrinos and right-handed  $W$  gauge bosons in final states with charged leptons and jets in  $pp$  collisions at  $\sqrt{s} = 13$  TeV with the ATLAS detector*, *Eur. Phys. J. C* **83** (2023) 1164, [[2304.09553](#)].
- [56] J. Blumlein, E. Boos and A. Kryukov, *Leptoquark pair production in hadronic interactions*, *Z. Phys. C* **76** (1997) 137–153, [[hep-ph/9610408](#)].
- [57] M. Schmaltz and Y.-M. Zhong, *The leptoquark Hunter’s guide: large coupling*, *JHEP* **01** (2019) 132, [[1810.10017](#)].

- [58] A. Bhaskar, A. Das, T. Mandal, S. Mitra and R. Sharma, *Fresh look at the LHC limits on scalar leptoquarks*, *Phys. Rev. D* **109** (2024) 055018, [[2312.09855](#)].
- [59] A. Alloul, N. D. Christensen, C. Degrande, C. Duhr and B. Fuks, *FeynRules 2.0 - A complete toolbox for tree-level phenomenology*, *Comput. Phys. Commun.* **185** (2014) 2250–2300, [[1310.1921](#)].
- [60] J. Alwall, R. Frederix, S. Frixione, V. Hirschi, F. Maltoni, O. Mattelaer et al., *The automated computation of tree-level and next-to-leading order differential cross sections, and their matching to parton shower simulations*, *JHEP* **07** (2014) 079, [[1405.0301](#)].
- [61] T. Sjöstrand, S. Ask, J. R. Christiansen, R. Corke, N. Desai, P. Ilten et al., *An introduction to PYTHIA 8.2*, *Comput. Phys. Commun.* **191** (2015) 159–177, [[1410.3012](#)].
- [62] A. Buckley, J. Ferrando, S. Lloyd, K. Nordström, B. Page, M. Rüfenacht et al., *LHAPDF6: parton density access in the LHC precision era*, *Eur. Phys. J. C* **75** (2015) 132, [[1412.7420](#)].
- [63] DELPHES 3 collaboration, J. de Favereau, C. Delaere, P. Demin, A. Giammanco, V. Lemaitre, A. Mertens et al., *DELPHES 3, A modular framework for fast simulation of a generic collider experiment*, *JHEP* **02** (2014) 057, [[1307.6346](#)].
- [64] T. Li, X.-D. Ma and M. A. Schmidt, *Implication of  $K \rightarrow \pi\nu\bar{\nu}$  for generic neutrino interactions in effective field theories*, *Phys. Rev. D* **101** (2020) 055019, [[1912.10433](#)].
- [65] A. J. Buras, J. Harz and M. A. Mojahed, *Disentangling new physics in  $K \rightarrow \pi\nu\bar{\nu}$  and  $B \rightarrow K (K^*) \nu\bar{\nu}$  observables*, *JHEP* **10** (2024) 087, [[2405.06742](#)].
- [66] V. Cirigliano, W. Dekens, J. de Vries, M. L. Graesser and E. Mereghetti, *Neutrinoless double beta decay in chiral effective field theory: lepton number violation at dimension seven*, *JHEP* **12** (2017) 082, [[1708.09390](#)].
- [67] KATRIN collaboration, A. Osipowicz et al., *KATRIN: A Next generation tritium beta decay experiment with sub-eV sensitivity for the electron neutrino mass. Letter of intent*, [hep-ex/0109033](#).
- [68] PLANCK collaboration, N. Aghanim et al., *Planck 2018 results. VI. Cosmological parameters*, *Astron. Astrophys.* **641** (2020) A6, [[1807.06209](#)].
- [69] KATRIN collaboration, M. Aker et al., *Direct neutrino-mass measurement based on 259 days of KATRIN data*, [2406.13516](#).